Evolution of basin architecture in an incipient continental rift: the Cenozoic Most Basin, Eger Graben (Central Europe)

Michal Rajchl,*·† David Uličný,‡ Radomír Grygar§ and Karel Mach¶

*Czech Geological Survey, Klárov 131/3, Praha 1, Czech Republic
†Institute of Geology and Palaeontology, Charles University, Praha 2, Czech Republic
‡Geophysical Institute, Czech Academy of Sciences, Praha 4,Czech Republic
§VŠB – Technical University Ostrava, Institute of Geological Engineering, Ostrava – Poruba, Czech Republic
¶Severočeské doly, a.s., Doly Bílina, Bílina, Czech Republic

ABSTRACT

The Oligo-Miocene Most Basin is the largest preserved sedimentary basin within the Eger Graben, the easternmost part of the European Cenozoic Rift System (ECRIS). The basin is interpreted as a part of an incipient rift system that underwent two distinct phases of extension. The first phase, characterised by NNE–SSW- to N–S-oriented horizontal extension between the end of Eocene and early Miocene, was oblique to the rift axis and caused evolution of a fault system characterised by en-échelon-arranged E–W (ENE–WSW) faults. These faults defined a number of small, shallow initial depocentres of very small subsidence rates that gradually merged during the growth and linkage of the normal fault segments. The youngest part of the basin fill indicates accelerated subsidence caused probably by the concentration of displacement at several major bounding faults. Major post-depositional faulting and forced folding were related to a change in the extension vector to an orthogonal position with respect to the rift axis and overprinting of the E–W faults by an NE–SW normal fault system. The origin of the palaeostress field of the earlier, oblique, extensional phase remains controversial and can be attributed either to the effects of the Alpine lithospheric root or (perhaps more likely because of the dominant volcanism at the onset of Eger Graben formation) to doming due to thermal perturbation of the lithosphere. The later, orthogonal, extensional phase is explained by stretching along the crest of a growing regional-scale anticlinal feature, which supports the recent hypothesis of lithospheric folding in the Alpine–Carpathian foreland.

INTRODUCTION

The relationships between the extensional stress field and an inherited basement fabric have a major influence on the geometry of fault arrays within rifts, and on the resulting geometries of sedimentary basins in rifts. In particular, the angle between the extension vector and the axis of a rift structure (typically a crustal-scale zone of mechanical weakness) is very important for the resulting three-dimensional (3D) geometry of rift-bounding faults and the resulting rift-basin geometry (e.g. Illies & Greiner, 1978; Tron & Brun, 1991; McClay & White, 1995; Morley, 1999; McClay *et al.*, 2002; Schumacher, 2002). Long-term evolution of rifted domains typically involves changes of stress fields through geologic time (e.g. Aldrich *et al.*, 1986; Ziegler, 1990; Doré *et al.*, 1997). This is reflected in overprinting of older fault systems by the new ones, resulting in compli-

cated structural geometries (Bonini *et al.*, 1997; Keep & McClay, 1997) not easy to interpret particularly in fossil rifts but also in recent rifts involving highly detailed data to elucidate the stress field history (Mortimer *et al.*, 2005). Another influence on the temporal evolution of rift basins is the growth and linkage of extensional faults, resulting in changes in the fault number and individual fault displacement, which in turn control temporal changes in basin subsidence (e.g. Cartwright *et al.*, 1995; Gupta *et al.*, 1998; Cowie *et al.*, 2000; Gawthorpe & Leeder, 2000; Morley, 2002). Understanding these controls on extensional fault geometries is important because of their influence on the positions of depocentres and their subsidence rates, as well as the tectonic topography governing the sediment dispersal paths, all critical factors for the distribution of hydrocarbon source and reservoir rocks (Scholz, 1995; Gawthorpe & Leeder, 2000; McClay *et al.*, 2002).

The Most Basin situated within the Eger Graben of Central Europe (Fig. 1) offers an opportunity to study the evolution of a fossil intra-continental extensional domain that features several distinct fault systems, with so far

Correspondence: Michal Rajchl, Czech Geological Survey, Klárov 131/3, 118 21 Praha 1, Czech Republic. E-mail: michal.rajchl@geology.cz
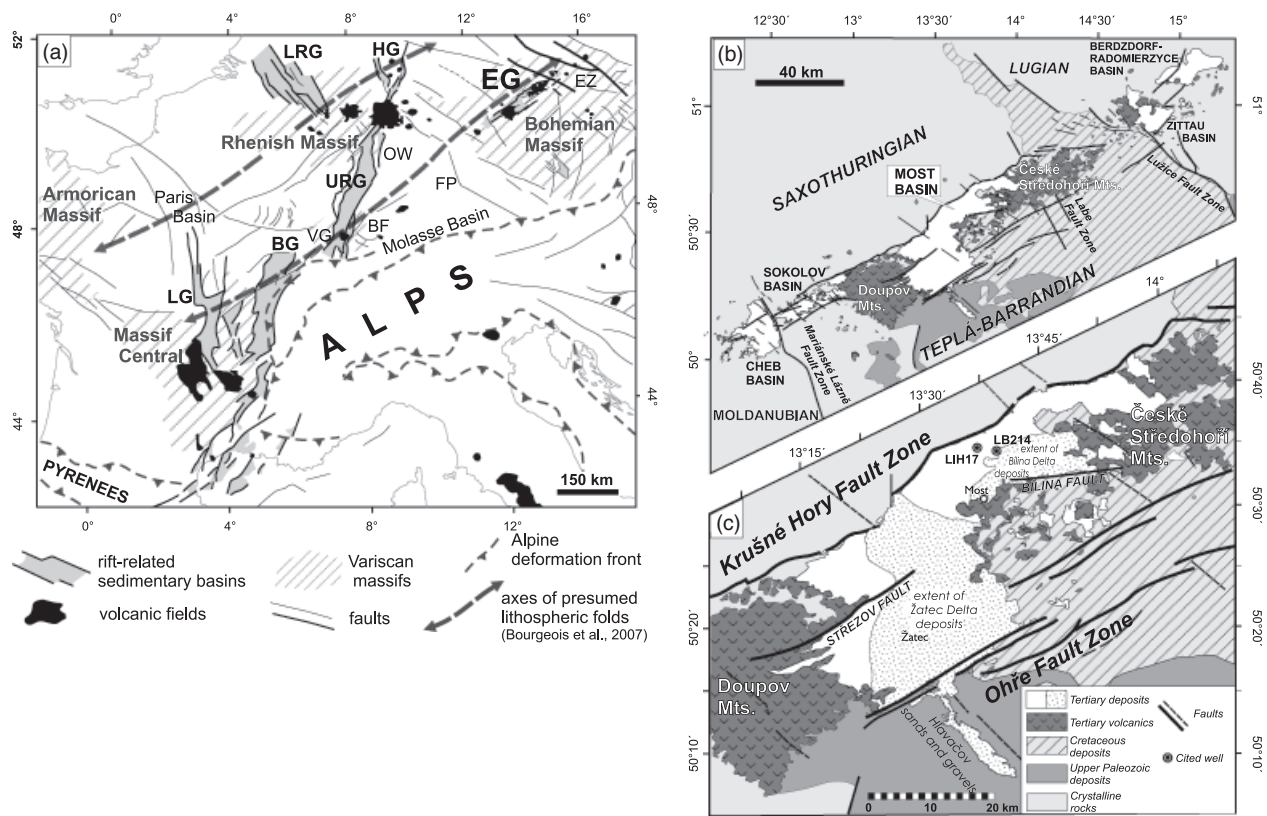
Fig. 1. (a) Schematic map showing the Eger Graben as a part of the European Cenozoic Rift System (ECRIS), modified after Dèzes *et al.* (2004). (BF, Black Forest; BG, Bresse Graben; EG, Eger Graben; FP, Franconian Platform; HG, Hessian grabens; EZ, Elbe Zone; LG, Limagne Graben; LRG, Lower Rhine (Roer Valley) Graben; OW, Odenwald; VG, Vosges) (b) A schematic geological map of the Eger Graben with the location of individual sedimentary basins and volcanic domains. (c) A schematic map of the Most Basin showing the present-day extent of clastic basin fill and coeval volcanics, and major tectonic structures.

poorly known spatio-temporal relationships between individual fault populations and the basin's depositional history. Špičáková *et al.* (2000) and Uličný *et al.* (2000) have suggested a significant role of oblique extension in the Eger Graben evolution, later replaced by orthogonal extension, but an understanding of the exact timing of these extensional phases and their relationship with post-rift deformation and uplift of this part of Alpine foreland requires analysis of new datasets. The Most Basin region offers a range of observational scales and types of data: (i) large-scale exposures of syntectonic strata in lignite mines; (ii) exposures of fault planes allowing mesoscopic structural observations to be made; (iii) dense regional borehole coverage; (iv) regional geophysical maps; and (v) several 2D seismic reflection lines combined with a wealth of subsurface and regional geophysical data.

The Eger Graben is the easternmost part of the European Cenozoic Rift System (ECRIS, Dèzes *et al.*, 2004), which is currently a subject of intense research and controversy regarding the causes and mechanisms of extension as well as post-rift deformation. Plume-related, collisional compression-driven or slab-pull-driven extension in the ECRIS are discussed, e.g., by Michon & Merle (2005) and Dèzes *et al.* (2005, and references therein). New data on tectonic evolution of the Eger Graben should also contribute towards a better understanding of the ECRIS dynamics.

GEOLOGICAL SETTING AND STRATIGRAPHY OF THE MOST BASIN

The NE–SW-oriented Eger Graben (Fig. 1) contains a higher volume of volcanics than most other ECRIS rifts. The lithosphere under the Eger Graben is thinned to *ca.* 80 km (Babuška & Plomerová, 2006), and the trace of the graben roughly parallels theNE–SW-trending depth contours of the Moho discontinuity, as shallow as *ca.* 30 km under the Erzgebirge (Krušné Hory) Mountains and deepening to the southeast (Dèzes *et al.*, 2004). The Eger Graben axis roughly parallels the trend of a major crustal boundary between the Saxothuringian and the Teplá-Barrandian zones of the Variscan orogen (Kossmat, 1927). This major crustal inhomogeneity, interpreted as a suture created during a major collisional event (Matte *et al.*, 1990), defined the northwestern border of the Late Palaeozoic post-orogenic extensional basin system in the Bohemian Massif (Jindřich, 1971; Malkovský, 1987). The post-rift history of the Eger Graben is dominated by deformation and erosion at its nortwestern flank during the Plio-Quaternary uplift of the Krušné Hory (Erzgebirge) Mts., up to *ca.* 1000 m elevations (cf. Zeman, 1988; Ziegler & Dèzes, 2007;Fig. 2).

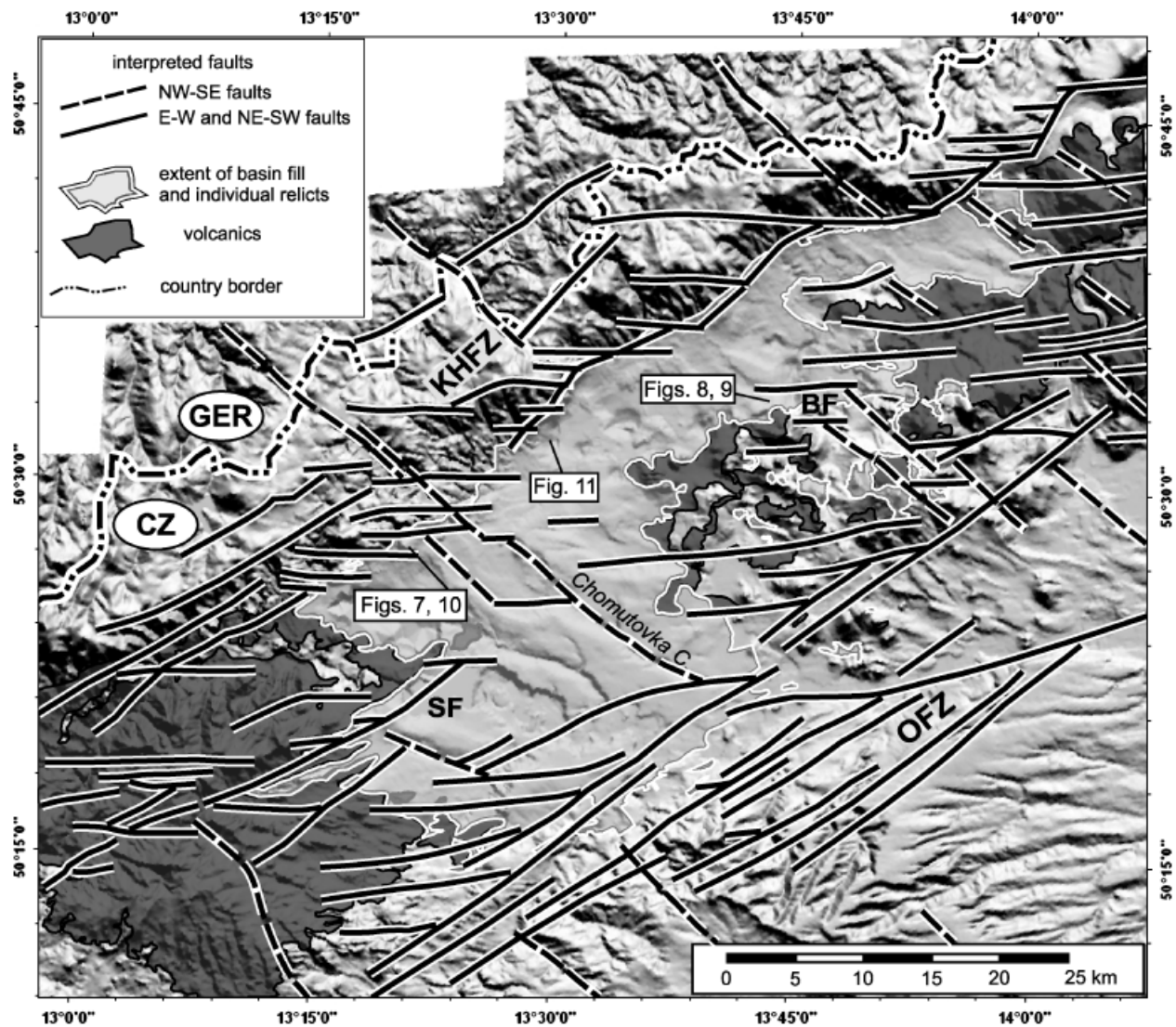The Most Basin is the largest of five sedimentary basins preserved within the Eger Graben (Fig. 1). The area of the

Fig. 2. Interpreted digital elevation model of the present surface of the Most Basin and its surroundings. Lines in the overlay mark tectonic structures displayed in the present-day topography. (BF, Bílina Fault; KHFZ, Krušné Hory Fault Zone; OFZ. Ohře Fault Zone; SF. Střezov Fault; CZ, Czech Republic; GER, Germany).

basin is *ca*. 1400 km^2 and the preserved basin-fill thickness reaches over 500 m (Fig. 3). The basin is bounded by the Krušné Hory Fault Zone, the Ohře Fault Zone and the Bílina Fault, together with the volcanic edifices Doupovské Hory Mts. and České Středohoří Mts. (Fig. 1). The pre-Cenozoic basement of the Most Basin is formed mainly by metamorphics of the Krušné Hory crystalline complex (Saxothuringian), and Upper-Proterozoic metamorphics of the Teplá-Barrandian domain (Mlčoch, 1994). Younger units that underlie parts of the Most Basin fill are Upper Palaeozoic sediments, volcanics and Cretaceous sediments (Malkovský *et al.*, 1985).

The onset of formation of the Most Basin and the entire Eger Graben is temporally associated with the onset of the main phase of volcanic activity in NW Bohemia during the latest Eocene (Kopecký, 1978; Cajz *et al.*, 1999; Ulrych *et al.*, 1999). The earliest part of the basin fill is the volcanogenic Střezov Formation, followed by clastics and carbonaceous deposits of the Most Formation (Figs 3 and 4).

Because of partial erosion of the stratigraphic record, the time of the end of syn-rift deposition in the Most Basin is not well known. It is inferred as latest early Miocene, based on magnetostratigraphy (Bucha *et al.*, 1987; Malkovský *et al.*, 1989) and palaeobotanical data (Teodoridis & Kvaček, 2006). The short lifespan and low subsidence rates in the Most Basin as well as other basins of the Eger Graben led Rajchl (2006) to interpret the Eger Graben overall as a failed, incipient rift.

DATA AND METHODS

Geophysical data

The map of horizontal gravity gradients was applied to investigate large-scale tectonic structures of the Most Basin that are covered by sediments and volcanics or overprinted by younger tectonic structures in the present topography.
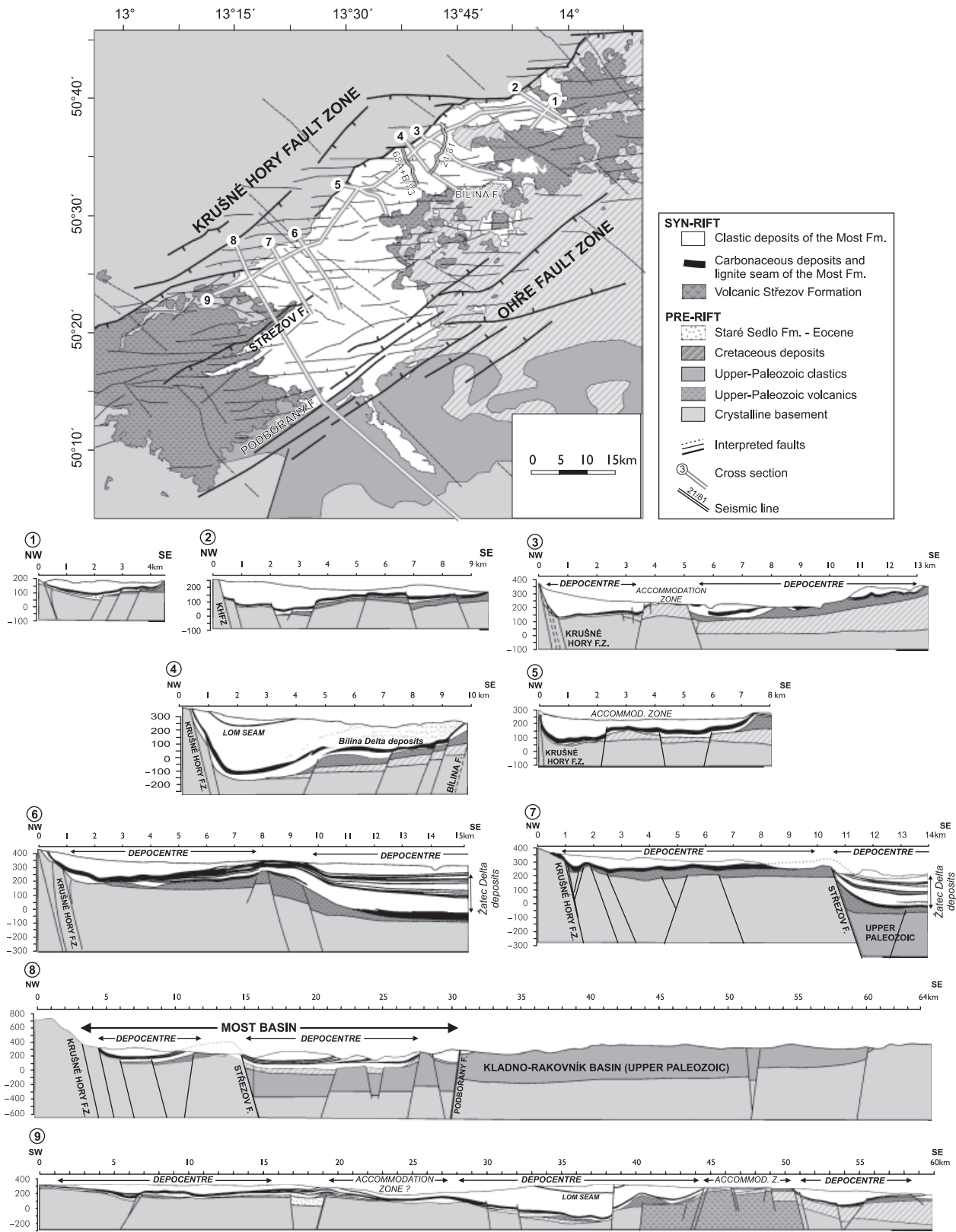
Fig. 3. Simplified geological cross–sections illustrating the geometry of the Most Basin fill were constructed based on archive proprietary data made available by Severočeské doly, a.s. The map shows the locations of individual cross–sections and seismic profiles from Fig. 6 within the fault pattern of the Most Basin.
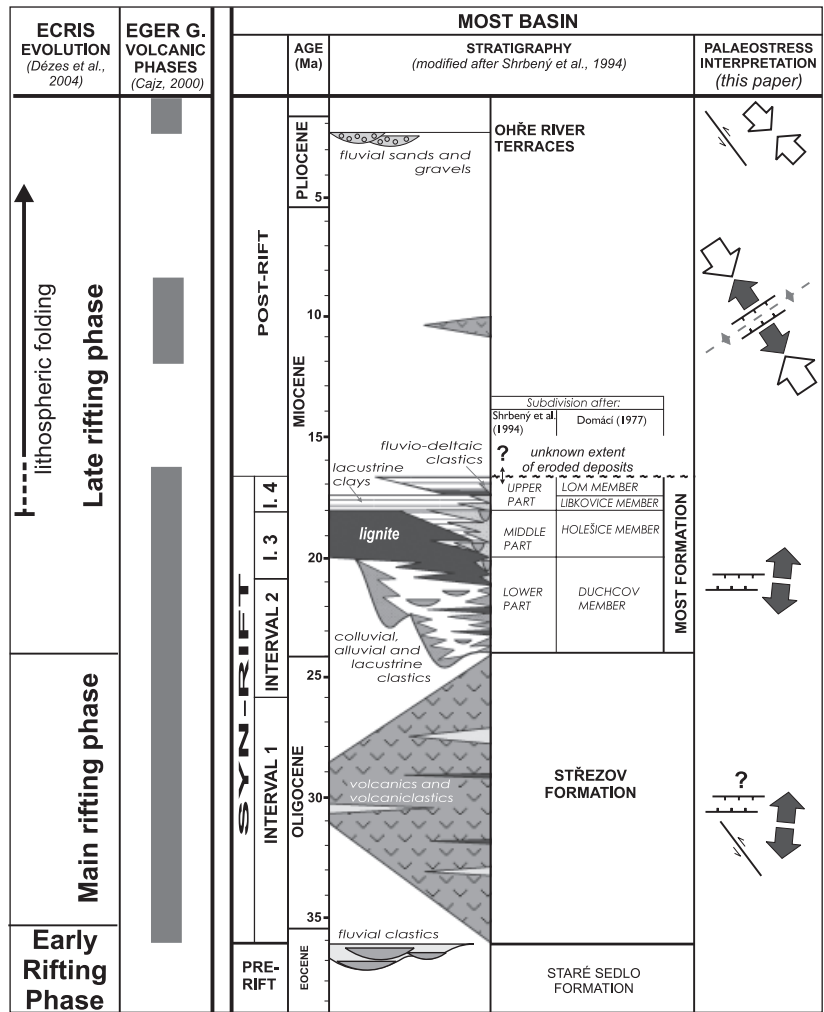
Fig. 4. Chart showing the regional stratigraphy of the Most Basin modified after Shrbený *et al.* (1994), with the alternative stratigraphy of Domácí (1977), together with the intervals of basin filling and interpreted palaeostress vectors, the temporal extent of Eger Graben volcanic phases (Cajz, 2000) and phases of the European Cenozoic Rift System (ECRIS) evolution (from Dèzes *et al.*, 2004).

Two seismic–reflection profiles were used to show a general picture of the basin–fill architecture and to clarify the problem of syn– vs. post–depositional tectonic deformation of the basin fill.

Borehole data

Archive borehole data were used for verification of the geological interpretation of seismic sections, construction of cross–sections and construction of isopach maps of the basin fill, to reconstruct the geometry of individual depocentres. Maps were constructed for the complete preserved basin fill and for three stratigraphic intervals: deposits overlying the main lignite seam, the main lignite seam and deposits underlying the main lignite seam. These intervals partially coincide with division of the Most Formation *sensu* Shrbený *et al.* (1994). The degree of precision of the maps depends on the depth and area of surface erosion of individual stratal units, and on the location and the number of boreholes used. The number of boreholes changes for individual intervals, because majority of the boreholes commonly did not reach below the lignite seam. A total of 587 boreholes were used.

Analysis of digital elevation model (DEM)

The reconstruction of the fault patterns, obtained by the methods mentioned above, was compared with a DEM of the present-day surface to identify traces of the tectonic structures in the present-day topography. This DEM was also used to map the youngest tectonic deformation of the Most Basin.

Sources of chronostratigraphic dating

Mostly palaeontological data were used to assess the timing of the basin filling (Kovar-Eder *et al.*, 2001), together with geochronological data from volcanic rocks of the České Středohoří Mts. (Bellon *et al.*, 1998; Cajz *et al.*, 1999). Ages based on palaeomagnetic data in Bucha *et al.* (1987) were used for comparison in the subsidence rate estimates.

Subsidence rate estimate

Lithological data from wells LIH-17 and LB-214, situated in the deepest part of the basin, spaced 3.8 km apart, and palaeomagnetically dated (Bucha *et al.*, 1987) were used for the estimate of the subsidence rate. They were com-

bined into a composite section, in order to represent the entire basin-fill record because one of the wells was not drilled to the basement. The section was decompacted using the standard backstripping procedure (Sclater & Christie, 1980), and the 'Decompact' spreadsheet by Waltham (2001) was used. Because of the absence of accurate chronostratigraphic data, two curves of decompacted depth to the basement were constructed, using different dating methods: (i) magnetostratigraphy (Bucha *et al.*, 1987) and (ii) palaeontological and radiometric data (Bellon *et al.*, 1998; Cajz *et al.*, 1999; Kovar-Eder *et al.*, 2001). Because of unconformities present in the well sections, the palaeomagnetic data could only be used as a crude proxy.

Structural analysis

Field-based structural analysis used mesotectonic data such as brittle faults, tension gashes, joints, etc., to verify or supplement the interpretations based mostly on large-scale fault array geometries and depocentre evolution. Reduced deviatoric palaeostress tensors were computed from cogenetic fault populations, in some cases separated from polyphase sets by evaluating field observation and kinematic compatibility. Such sets were analysed with the P–T-axis method (Peresson, 1992) and, where necessary, compared with the numerical dynamic analysis (NDA) method (Sperner *et al.*, 1993) using the software package TectonicsFP 1.6.2 (Reiter & Acs, 2002). Both the P- and T-axes and the NDA-method give kinematic axes that, in case of coaxial deformation, are considered to coincide with the principal stress axes σ_1, σ_2 and σ_3.

ARCHITECTURE OF THE MOST BASIN

Fault systems

The most prominent in the present-day topography of the Most Basin is the NE–SW fault system, basically aligned with the Eger Graben axis (Fig. 1). Rajchl & Uličný (2000), Uličný *et al.* (2000), and Špičáková *et al.* (2000) demonstrated that the Eger Graben basins were strongly controlled by two other faults systems during the basin evolution. These are represented by E–W-oriented faults and NW–SE-trending faults.

E–W fault system

The E—W- to ENE–WSW-striking faults are mostly short in length (5–10 km locally), show small displacement (50–200 m) and occur abundantly in the entire basin. Although only locally well exposed, they are shown clearly in the map of horizontal gravity gradients (Fig. 5). The generally E–W-oriented gravity gradients are identified as shallow crustal faults, based on their correlation with seismic profiles and borehole data (Figs 3 and 6). The distribution of some of the E–W faults is also demonstrated in the DEM of the Most Basin basement (Mlčoch & Martínek, 2002). The analysis of the DEM of the present-day surface

shows a number of E–W-trending structures within the topography of areas surrounding the Most Basin (Fig. 2). In the present-day topography of the Most Basin, the E–W fault system is represented mainly by E–W-oriented segments of the Krušné Hory Fault Zone and the Bílina Fault. Numerous E–W faults probably functioned as volcanic pathways and were sealed and covered by volcanics (cf. structural data in Cajz, 2001). E–W-trending fabrics have been described from the Saxothuringian basement metamorphics of the NW periphery of the Most Basin (Konopásek *et al.*, 2001). In the southeastern part of the Eger Graben, where the Cenozoic strata are underlain by Cretaceous and Upper Palaeozoic sediments, inherited basement E–W structures have not been reported.

The fault segments are arranged in an en-echélon pattern in plan view (Fig. 5) and some tend to be curved into parallelism with the basin axis. The en-echélon pattern results in abundant relay ramps separating individual fault segments (e.g. Peacock & Sanderson, 1994; McClay & White, 1995).

The most accessible example of this fault system is the Bílina Fault (Fig. 8), which is recognised by Váně (1985a) as a part of an en-echélon fault array. The fault is characterised by overlapping segments up to 10 km long, and accompanied by a fault-propagation fold, marked by deformation in the prominent lignite seam. The maximum vertical throw on the Bílina Fault segment 1 (Fig. 9) is *ca*. 190 m. In the immediate vicinity of the large-scale Bílina Fault, several populations of small-scale normal faults occur. The population of roughly E–W-trending, oblique normal faults, with a moderate dextral component, and less abundant, dextral shear trending roughly NE, is assumed to be syn-kinematic with the Bílina Fault (Fig. 9a) because it occurs within the trace of the Bílina Fault. Fault populations of other orientations are considered younger and are discussed further below.

A similar set of phenomena is observed at the northern basin margin, at an exposed example of the E–W fault segments within the Krušné Hory FZ characterised by a normal to a slightly oblique normal displacement (Fig. 10).

Timing of the E–W fault system activity: Large-scale fault geometry as well as mesoscopic data indicate NNE-directed extension as causing the activity of this fault system. Direct field evidence of the syn-sedimentary effects of these faults is limited, but could be well represented by two examples of syn-sedimentary forced folding above propagating fault segments (Figs 8 and 10). In both cases, basinward divergence of sedimentary strata recorded tilting of depositional surface above an upward-propagating segment of a normal fault (cf. Gupta *et al.*, 1999).

Along the northwestern edge of the preserved basin fill, Oligo-Miocene coarse-grained clastics, including gneiss boulders, were interpreted by Váně (1985a) as colluvial deposits, suggesting that the Krušné Hory FZ already operated as a syn-sedimentary tectonic margin of the Most Basin. It is, however, likely that the active faults were the E–W segments, the relics of which are still present as
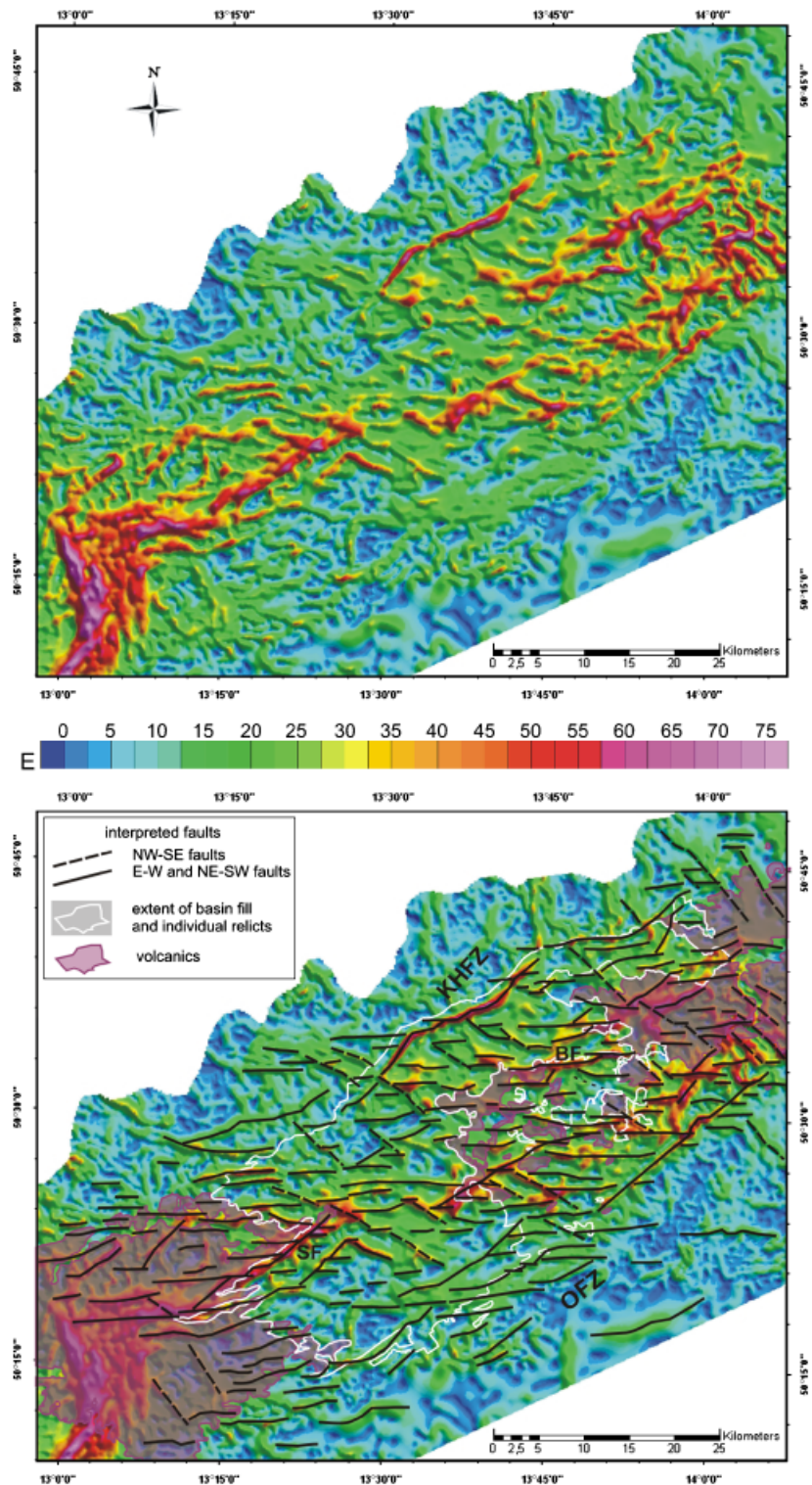
Fig. 5. (a) Uninterpreted and (b) interpreted map of horizontal gravity gradients of the Most Basin and the surrounding area. The map was produced by Geofyzika, a.s., Brno and Miligal, s.r.o., compiled from regional gravity mapping on a 1 : 25 000 scale, using reduction density 2.30 g cm^{-3}, with illumination from N30E. The black lines in (b) mark those horizontal gravity gradients interpreted as fault structures. The fault pattern is represented by E–W, NE–SW and NW–SE fault systems. The high gradients in the southwestern corner of the map correspond to the edge of Variscan granitoids underlying the Cenozoic volcanics of the Doupovské Hory Mts. (BF, Bílina Fault; KHFZ, Krušné Hory Fault Zone; OFZ, Ohře Fault Zone; SF, Střezov Fault).

parts of the Krušné Hory FZ. The clastics most likely entered the basin *via* relay ramps present in the locations of the small clastic bodies. The fluvial deposits of the Hradiště locality occur on a preserved relict relay ramp, and show palaeocurrents towards the south (Fig. 7). Also, the sand bodies, documented by Elznic (1963), Elznic *et al.* (1998), Váně (1961) and Zelenka & Polický (1964) within the lignite seam and overlying lacustrine deposits along the northwestern edge of the preserved basin fill, were probably deposited by fluvio-deltaic systems entering the basin through relay ramps.

The syn-sedimentary activity of this fault system is also supported by seismic reflection data that show small-displacement normal faults of E–W orientation, commonly terminated within the main lignite seam and resulting in its local flexure (Fig. 6). This suggests that the activity of these faults ceased early during the basin evolution and only major, graben-bounding faults remained active.
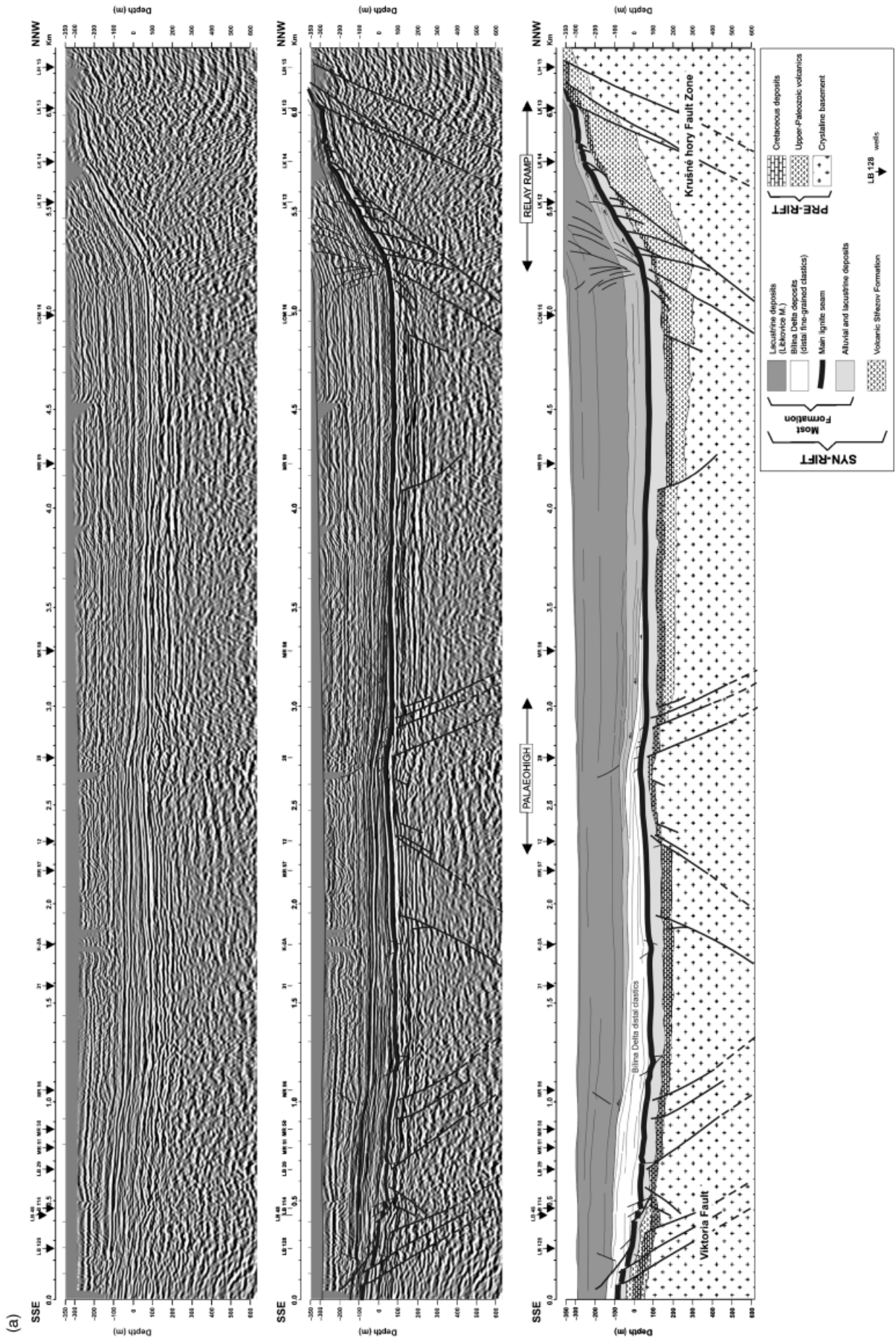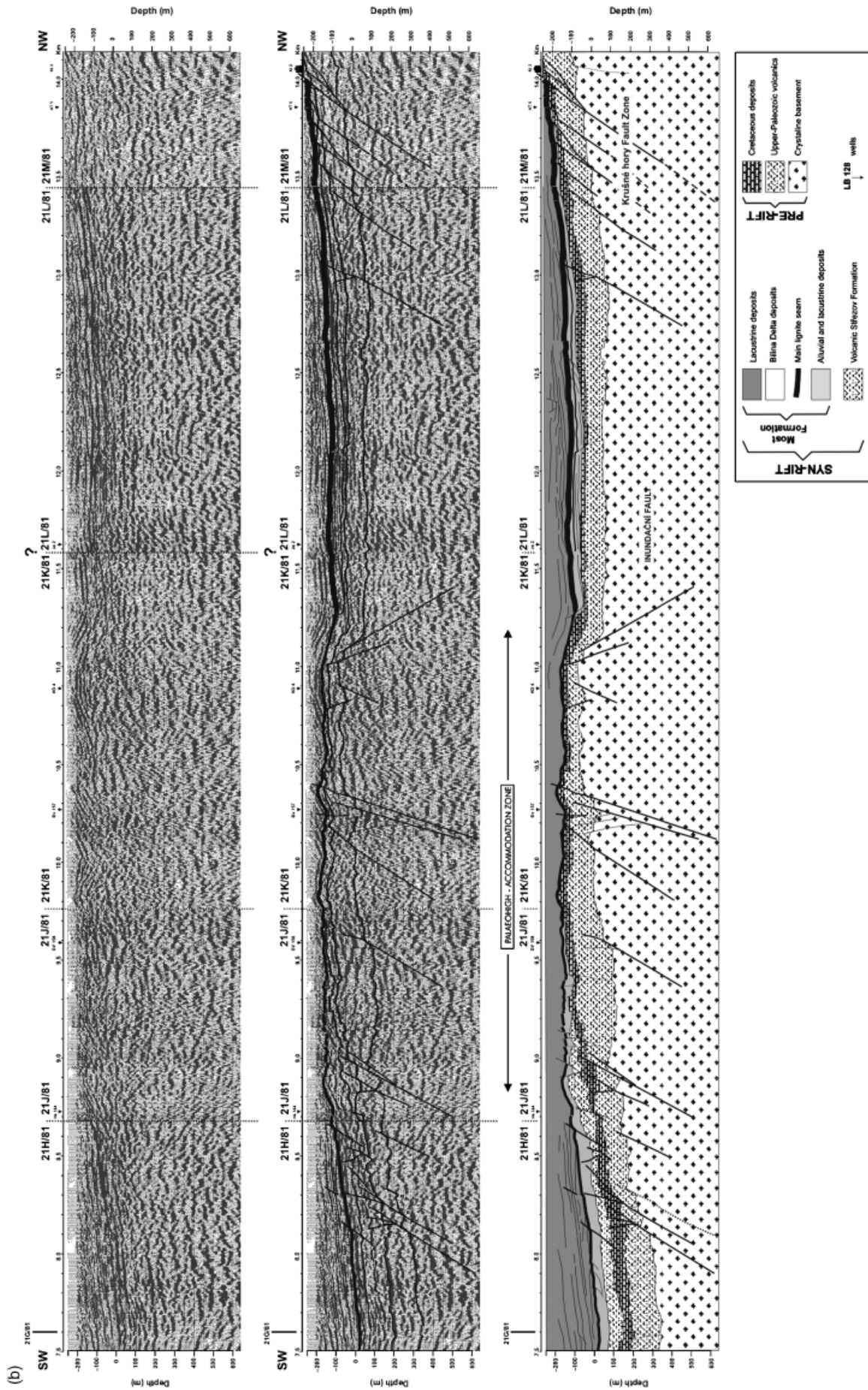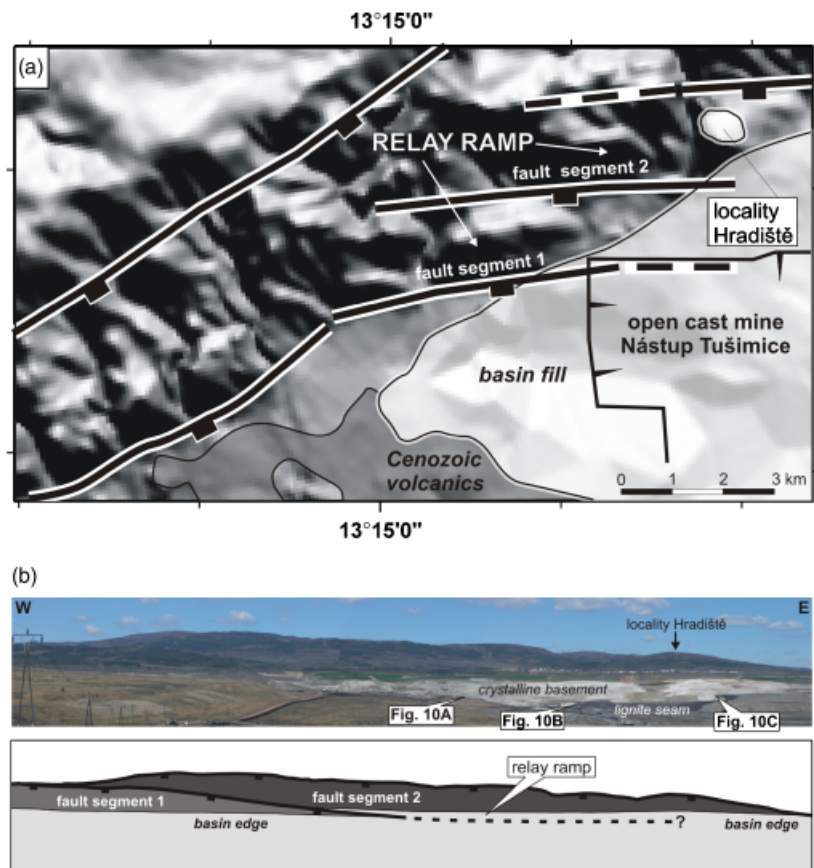
Fig. 7. (a) Interpreted digital elevation model and (b) panorama of the faulted NW margin of the Most Basin (Krušné Hory FZ). The images show E—W-oriented fault segments separated by relay ramps. A relict of a fluvial clastic body (the locality Hradiště) suggests the syn-depositional activity of the ramp that functioned as a south-directed pathway of clastics into the basin. For location, see Fig. 2.

NE–SW fault systems

Normal faults of NE–SW orientation, showing typically greater lengths than the E–W faults, represent the most prominent structural trend in the topography of the Most Basin, parallel to the axis of the Eger Graben (Figs 1 and 2). However, a marked spread of directions between *ca*. N35E and N60E is observed in this group of faults. Locally, some NNE-trending fault populations contain faults aligned nearly N–S. Within the entire Eger Graben, the fault system is represented by parts of the Krušné Hory Fault Zone and the Ohře Fault Zone at the present-day southeastern graben margins. Within the Most Basin, few major faults follow this trend (Fig. 2).

A significant morphological feature of the Krušné Hory Fault Zone is the kinked trace of the faults, characterised by a number of relatively short E–W-trending fault segments, commonly linked by short segments of nearly NNE–SSW strike (Fig. 2). It is evident that the Krušné Hory Fault Zone is a complex structure, represented in some places by normal fault segments (Fig. 3, cross-sections 2, 3) and elsewhere by monoclinal folding of the basin-fill strata in relicts of relay ramps (Fig. 3, cross-sections 5–7; cf. Malkovský, 1979; Hurník & Havlena, 1984; Marek, 1985). On the opposite margin of the Most Basin, the Ohře Fault Zone is represented by several relatively straight-, parallel-trending NE–SW faults (15–30 km long) and by a number of small fault segments, as shown in the

Fig. 6. Reflection seismic profiles 68/83 (a) and 21/81 (b), recently reprocessed by Geofyzika, a.s., Brno and reinterpreted (Uličný & Rajchl, 2002; Rajchl *et al*., 2003a, b; see Jihlavec & Novák, 1986 for original interpretation), showing the architecture of the basin fill within the Bílina depocentre. (a) Profile 68/83 shows a number of important phenomena: (i) an extensional horst-like structure (of relief up to 100 m) interpreted as an accommodation zone that separated two small grabens during the initial stage of the basin evolution and became inactive after the main seam deposition (location between 2.3 and 3 km); (ii) wedge shape and shingle-like internal architecture of distal parts of the Bílina Delta; (iii) the effect of peat compaction on accommodation creation for the earliest lacustrine deposits, NW of 2.5 km. The thickness of the lowermost part of the lacustrine deposits shows an inverse relation to the thickness of underlying deltaic clastics. The lacustrine deposits are the thickest in places where the deltaic clastics are absent; (iv) onlap of lacustrine strata on the surface of the Bílina Delta sedimentary body suggests gradual drowning of the deltaic sedimentary system; (v) post-depositional fault-propagation folding of the basin fill close to the NW margin of the basin. (b) Part of the profile 21/81 (segments H, J, K, L, M), showing a large horst-like structure between 8.5 and 11.4 km, defined by normal faults and interpreted as an accommodation zone. This syn-depositional structure is characterised by a reduction in the coal seam thickness (locally down to 1.5 m) and underlying deposits (including volcaniclastics). A number of normal faults affecting the deposits underlying the main lignite seam and partly the main lignite seam are evident in both (a) and (b). See the map in Fig. 3 for the location of the profiles.
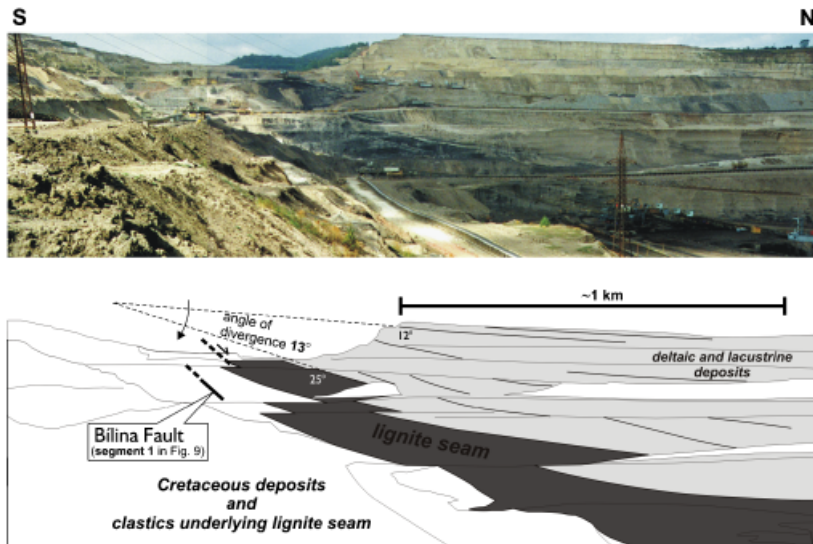
Fig. 8. Deformation of the main lignite seam and clastics of the Bílina Delta along the Bílina Fault – southern margin of the Bílina open cast mine (as of 2000). The clastic wedge of the Bílina Delta prograded generally westward, aligned with the active segments of the Bílina Fault (Rajchl *et al.*, 2008). Basinward divergence of deltaic and lacustrine strata suggests syn-depositional tilting of a sedimentary surface caused by fault propagation folding. Local divergence between the top of lignite seam (25°) and palaeohorizontal markers within the uppermost deltaic clastics (12°) is 13°. The location of Fig. 8 in Figs 2 and 9 shows the position of the uppermost terrace of the mine.

data of Hradecký (1977), Malkovský (1979) and Malkovský *et al*. (1985).

The Střezov Fault represents the only significant intra-basinal fault of the NE–SW direction and divides the widest part of the basin into two parts (Figs 1 and 2). This fault is *ca*. 25 km long and its SW tip terminates in the centre of the Doupovské Hory volcanic complex. In the basement, the trace of this fault generally coincides with the position of the faulted margin of the Permo-Carboniferous Kladno-Rakovník Basin (Mlčoch & Martínek, 2002; Fig. 3 – cross-sections 7, 8).

Timing of the NE–SW fault system activity: The Krušné Hory FZ (Figs 1, 2 and 5) was formed by linkage of short segments of the E–W fault system across their relay ramps, and as a whole, is clearly younger that the E–W faults. It is, however, not completely clear whether the linkage occurred only after the deposition in the basin had ceased or whether it had already occurred during the younger depositional phases. The presumed syn-depositional existence of the Krušné Hory FZ as one of the main syn-rift 'deep faults' (e.g. Kopecký, 1978) has been disproved long ago (Váně, 1985a), but this assumption is still found implicitly or explicitly in some recent literature (Michon *et al.*, 2003). NE- to NNE-trending segments of the Krušné Hory Fault Zone suggest a roughly NW-directed extension; it is discussed below whether this represents a regional palaeostress field or an evolution of a local stress field between propagating E–W fault tips that led to relay ramp breaching.

Post-depositional displacement along the Ohře FZ is documented by faulting of the entire basin fill and by relicts of Neogene strata in post-depositional grabens southeast of the Most Basin border. The large thickness of fluvial clastics of the so-called Žatec Delta (Fig. 3, cross-sections 6–8) indicates that syn-depositional accommodation existed in the area of the Ohře FZ during the lignite seam formation. It is unclear, however, whether the active faults had the same strike as the present-day NE–SW structures – this also applies to the presumed faults further southeast that governed the formation of

the lower Miocene hot-spring freshwater limestones of Tuchořice (Váně, 1985a; Fejfar & Kvaček, 1993). The faulted margin of the basin in the Žatec Delta area apparently did not function as the syn-depositional basin edge. Indices of E–W-trending structures occur in the gravity gradient maps, marking possible unmapped, E–W-trending, precursors of the later Ohře FZ.

In addition to undoubted post-depositional displacement, Neogene-age syn-sedimentary activity of the intra-basinal Střezov Fault is documented by the change in the thickness of Neogene clastics between the footwall and the hangingwall blocks (Fig. 3 – cross-section 7). The unchanged thickness of Střezov Formation volcanics across the fault (Malkovský, 1979) and the absence of clastics underlying the main lignite seam on the hangingwall side of the fault, together with the architecture of the seam (Fig. 3 – cross-sections 7, 8), suggest that the NE–SW Střezov Fault began to be active during the seam evolution.

Other, minor faults of SSW–NNE occur in various places within the basin and generally show post-depositional normal displacement in NW-directed extension, such as the Eliška Fault (Fig. 11; Brus & Hurník, 1987). Mesoscopic brittle structures along the Bílina Fault (Fig. 9a) suggest that, in addition to the syn-depositional E–W-trending normal faults, another population of mesoscopic faults occurs, trending NE–SW to NNE–SSW, and shows normal displacement with a weak sinistral component. This population, occurring pervasively both in the footwall and in the hangingwall of the Bílina Fault Segment 1 (Fig. 9), indicates local NW–SE-directed extension. Post- vs. syn-depositional age of these faults with respect to the seam and clastics in the Bílina Fault hangingwall cannot be determined with certainty. In addition, localised sets of fault–slip data are not sufficient for determining a larger-scale palaeostress field (e.g. Gapais *et al.*, 2000).

NW–SE fault system

Both the DEM (Fig. 2) and the horizontal gravity gradients (Fig. 5) indicate that the Most Basin is significantly af-
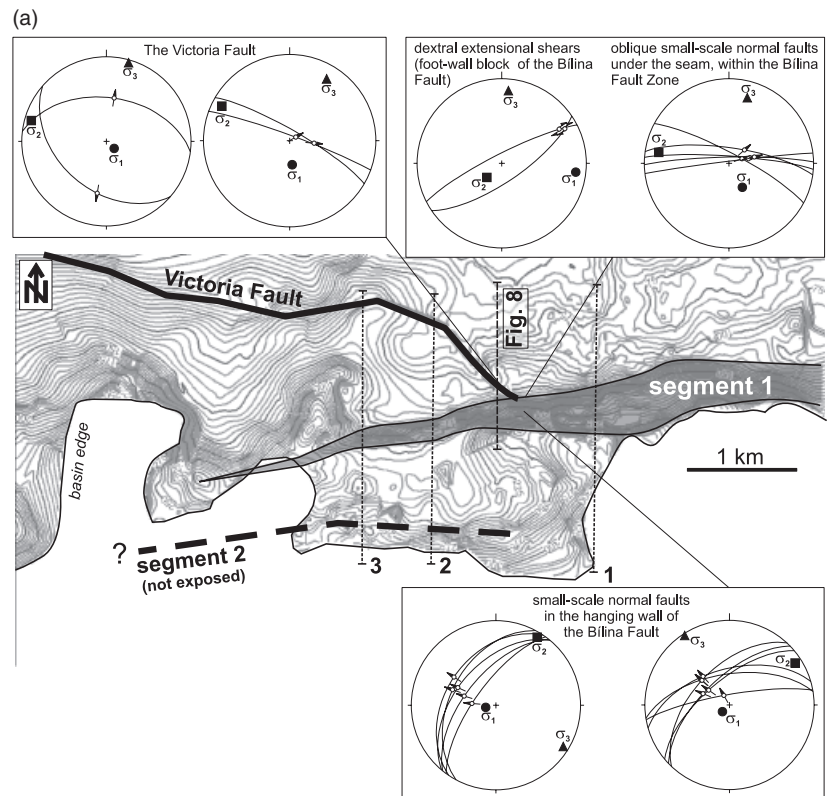
Fig. 9. (a) A structural map showing the elevation (in metres above the sea level) of the base of the main seam in the vicinity of the Bílina Fault (location in Fig. 2). The contour lines illustrate the displacement associated with one of the en-echélon segments of the Bílina Faults (Segment 1 in the figure), including the fault-propagation fold accompanying it, and the topography of the relay ramp between fault segments 1 and 2. The interpretation of meso-scale structural data is shown to illustrate the details of fault kinematics. 'Basin edge' refers to the present-day erosional edge of preserved basin fill. (b) Changing vertical displacement along segments 1 and 2 is illustrated by cross sections highlighting the two-dimensional geometry of the main lignite seam close to the Bílina Fault.
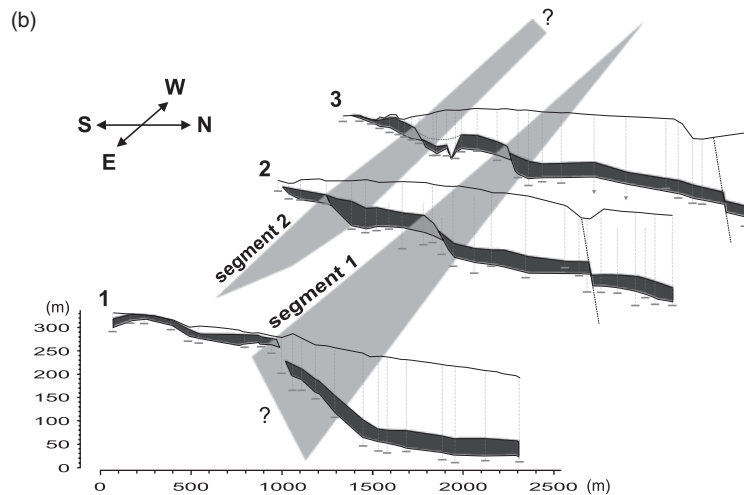
fected by a number of NW–SE-trending faults occurring as 20–30-km-long segments. Several faults close to the NW–SE orientation were also detected by mining (Malkovský, 1979; Malkovský *et al*., 1985; Brus & Hurník, 1987). A number of faults of similar orientation are documented in other basins of the rift (Kasiñski, 2000; Špičáková *et al*., 2000; Rojík, 2004). Apart from the straight, near-vertical,

clearly basement-derived faults of NW–SE strike that cross the entire basin (Fig. 2), some intra-basinal faults trend NW–SE only along a part of their trace. An example is the Victoria Fault recently exposed in the Bílina mine (Fig. 9) locally curved from a nearly E–W strike to a pure NW strike. A WNW-trending segment of this fault was exposed where it joins the Bílina Fault and shows normal to

Fig. 10. Deformation of basin fill associated with the activity of segment 1 of the Krušné Hory FZ from Fig. 7 (see also Fig. 7 and 2 for location). (a) A closeup view of an E–W fault segment of the Krušné Hory FZ juxtaposing the basin fill against the crystalline basement in the footwall. The fault is characterised by normal to slightly oblique normal displacement. (b), (c) Two examples of syn-depositional forced folding above the propagating E–W fault segment of the Krušné Hory FZ. In (b), the trace of base of the lignite seam shows apparent curvature due to a curved quary wall. Subtle basinward divergence of sedimentary strata recorded tilting of the depositional surface above the upward-propagating normal fault segment. The apparent divergence angle is decreased due to differentcial compaction above surface A – note the transition from mudstones to lignite in the basinward direction.
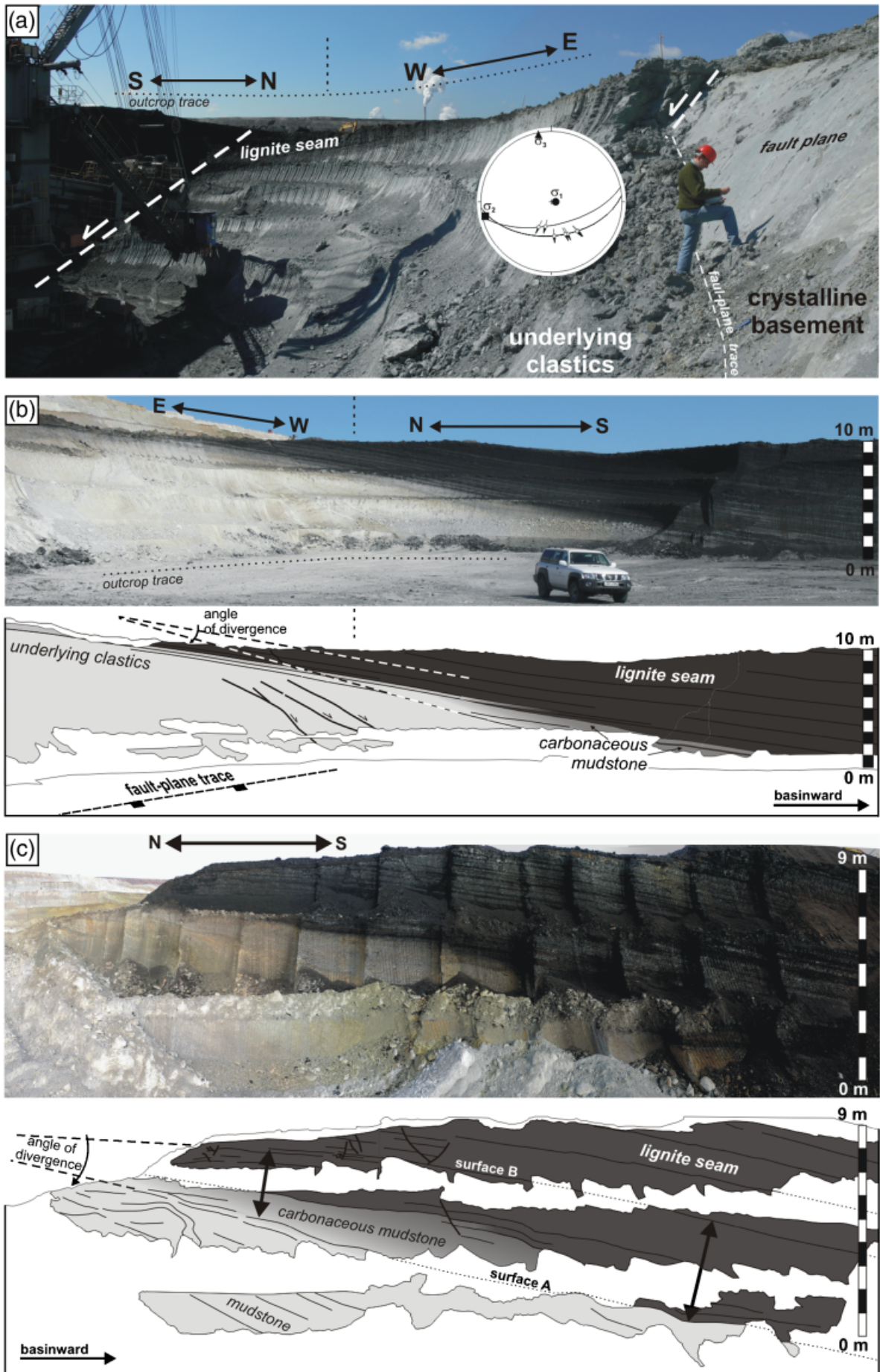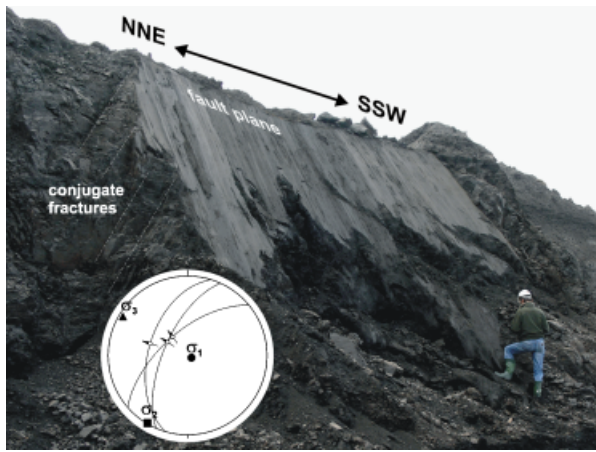
Fig. 11. A photograph of the Eliška Fault, one of the minor SSW–NNE faults showing generally post-depositional normal displacement in NW-directed extension. For the location of the photograph, see Fig. 2.

slightly dextral displacement (Fig. 9a), similar to the Bílina Fault mesoscopic data. The trace of the Victoria Fault (Fig. 9) shows that the fault is a composite structure formed by linkage of former E–W fault segments. Seismic profile 68/83 documents syn-depositional vertical displacement on an E–W segment of the Victoria Fault.

Timing of the NW–SE fault system activity: The NW–SE orientation of the faults essentially coincides with the trend of the Elbe Zone, one of the significant shear zones formed during the Late Palaeozoic Variscan orogeny (Arthaud & Matte, 1977; Schröder, 1987; Scheck *et al.*, 2002) (Fig. 1a). The existence of this pre-rift fault system significantly affected the geometry of later fault systems that formed during opening of the Eger Graben. Bending of some of the E–W faults to parallelism with the NW–SE faults suggests their coeval activity. Post-depositional vertical displacement of several tens of metres is documented at the NW-trending segment of the Victoria Fault (Fig. 9). No mesoscopic data were found to assess the kinematics of these faults during the basin filling; a sinistral strike–slip regime is interpreted for their post-rift, Pliocene phase of activity in peripheral parts of the Eger Graben (Cheb Basin, e.g. Špičáková *et al.*, 2000; Pliocene volcanics at the Lužice Fault Zone; R. Grygar, unpublished data). Geomorphological data suggest a possible narrow, sinistral pull-apart structure with a Pliocene to Quaternary infill following the faults of the Chomutovka Creek (Fig. 2), so far not proven by independent methods. The dextral component of slip in the Victoria Fault zone (Fig. 9a) is probably due to its merging with the Bílina Fault segment 1 in the location of measured exposure, where the data correspond to the kinematics of the E–W normal faults.

Some of the NW–SE faults served as a pathway for clastics transported into the area of the Žatec Delta close to the southeastern margin of the basin (Fig. 1). This clastic belt is known as the Hlavačov gravels and sands (e.g. Váně, 1985a) and is characterised by a 'panhandle' map-view

shape (by analogy to the 'panhandle' of the Okavango inland delta in Botswana, e.g. McCarthy *et al.*, 1992).

Most Basin depocentres: geometry and spatial arrangement

Four main depocentres of the basin are distinguished based on preserved basin-fill geometry (Rajchl, 2006; Figs 12 and 13). However, a number of small basin-fill relicts suggest that the area of deposition exceeded the present-day limit of the basin. The depocentres are elongate and show a graben or a half-graben geometry in cross-section (Figs 3 and 6). The Chomutov, Bílina and Teplice Depocentres are arranged in an en-echélon pattern, similar to their bounding E–W fault segments. The Žatec Depocentre axis has a NE–SW orientation (Fig. 13). The depocentres are separated from one another by palaeo-highs (Fig. 12), characterised by reduction of the thickness of the basin fill (Fig. 3 – cross-section 9; Fig. 6b). Only in the case of the Žatec and Chomutov Depocentres is the separation partially caused by the Střezov Fault (Fig. 3 – cross-section 8; Fig. 13).

The orientation and geometry of the palaeohighs with respect to individual depocentres suggest their function as accommodation zones (cf. Peacock *et al.*, 2000; McClay *et al.*, 2002). The orientation of the accommodation zones roughly coincides with the transverse, NW–SE trending, basement faults (Fig. 13) that probably defined their position and the offset of individual depocentres (for similar observations, see, e.g., Le Turdu *et al.*, 1999; Morley, 1999; McClay *et al.*, 2002).

Cross-sections and isopach maps (Figs 3, 6 and 12) show that the size and shape of the depocentres changed significantly during the Most Basin evolution. The data document the gradual linkage of small initial depocentres, eventually merging into the four large depocentres defined above (e.g. Fig. 6a). The initial depocentres were only a few square kilometres across (Fig. 12).

TECTONOSEDIMENTARY EVOLUTION OF THE MOST BASIN

Intervals of basin filling

Interval 1: volcanics and volcaniclastics (latest Eocene–Oligocene, 36–26 Ma)

During the first depositional interval, the Most Basin was filled by the volcanosedimentary Střezov Formation (Fig. 4) comprising alkaline volcanics close to the volcanic centres, and pyroclastics and redeposited pyroclastic material in the initial depocentres (e.g. Domácí, 1977; Malkovský *et al.*, 1985). The single NW-elongated thickness maximum shown in Fig. 12a is probably caused by Eocene clastic infills of inherited topography that pre-date the volcaniclastic deposition but in archive borehole documentation are mostly impossible to distinguish from the volcaniclastics. Other deposits of the Střezov Formation include intercalations of lacustrine limestones, diatomites
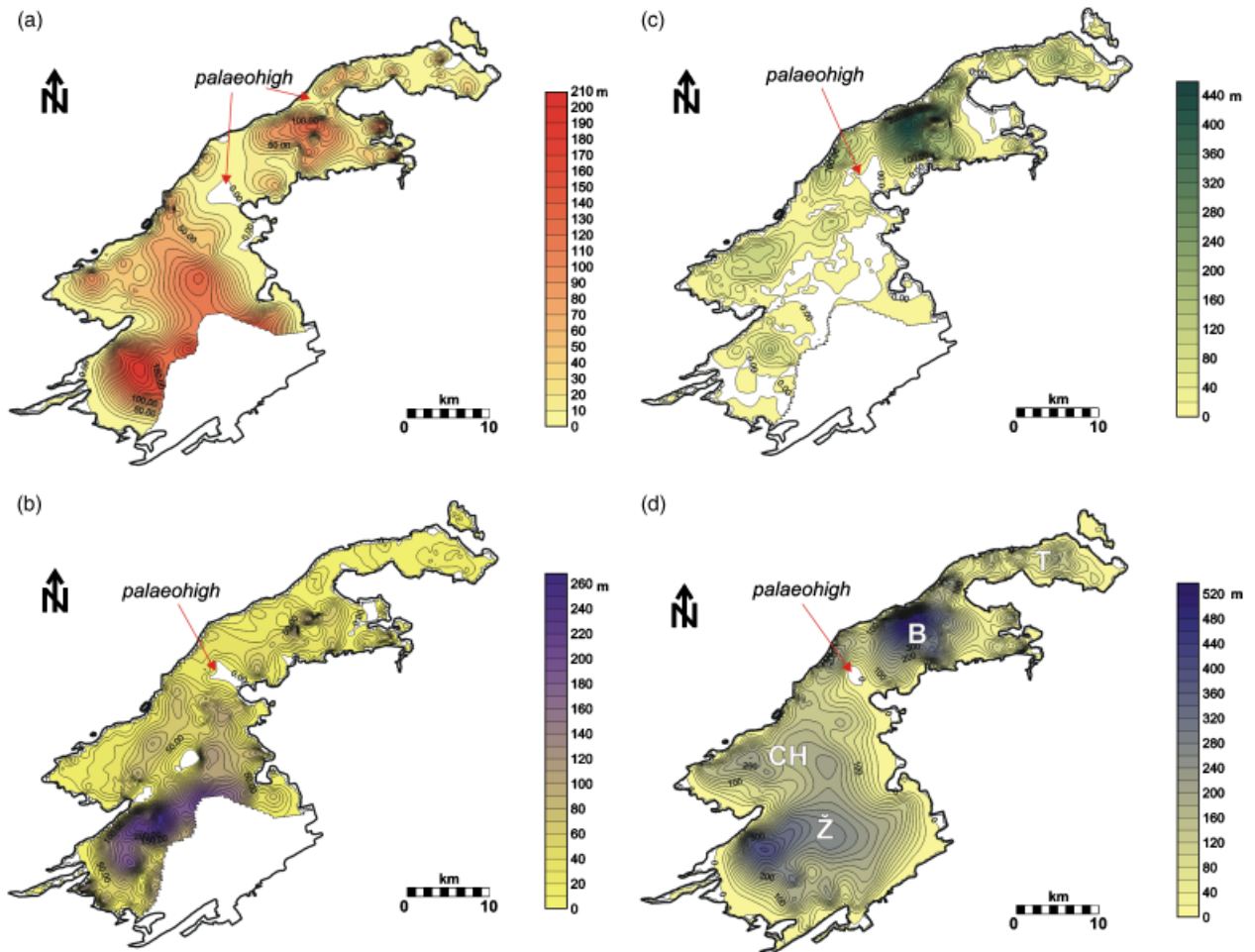
Fig. 12. Isopach maps of the Most Basin fill. (a) Thickness of volcanics and clastics underlying the main lignite seam. (b) Thickness of the main lignite seam and coeval clastics. The thickness of lignite is displayed without decompaction, which causes a significant increase of the thickness towards places with clastic interbeds. (c) Thickness of lacustrine deposits overlying the main lignite seam. (d) Total thickness of the basin fill. (B, Bílina Depocentre; CH, Chomutov Depocentre; T, Teplice Depocentre; Ž, Žatec Depocentre). Borehole data were obtained from Geofond of the Czech Republic and the archive of Severočeské Doly, a.s.

and carbonaceous clays or coals, deposited in lacustrine and swamp environments (e.g. Domácí, 1977; Malkovský *et al.*, 1985; Bellon *et al.*, 1998). Cajz (2000) correlates the Střezov Formation with the lower stratigraphic unit of the volcanic České Středohoří Mts. (36–26 Ma) that fills the original topography and the initial depocentres of the incipient rift structure. Curves of subsidence rate evolution (Fig. 14) show very low subsidence rates during this stage of the basin evolution, on a scale of a few m Ma^{-1}.

Interval 2: clastics under the main seam (latest Oligocene–earliest Miocene, 26–21 Ma)

Proluvial and alluvial deposition of material derived from the surrounding volcanics and the Cretaceous and crystalline basement dominated during this interval of the basin evolution, corresponding to the lower part of the Most Formation (Fig. 4; e.g. Malkovský *et al.*, 1985). Local lacustrine and coal-bearing environments also formed within the depressions of newly forming relief (e.g. Malkovský *et al.*, 1985;

Elznic *et al.*, 1998). The cross-sections and isopach maps show that the small local depocentres were formed generally along the present-day Krušné Hory Fault Zone, controlled by a number of minor intra-basinal normal faults of small displacement (Fig. 6). The geometry of the depocentres and the correlation of seismic and lithological cross-sections to the mapped fault framework suggest that the topography of the Most Basin area was generally affected by an E–W-oriented fault system during this stage of the basin evolution (Fig. 15a). Subsidence curves indicate a modest increase of the subsidence rate in the central part of the basin during this phase (Fig. 14). The thickness of the corresponding deposits, shown by cross-sections (Fig. 3), suggests that the subsidence rate could locally exceed 10 m Myr^{-1}.

Interval 3: main lignite seam and corresponding clastics (early Miocene, 21–18 Ma)

This interval is represented by the main lignite seam in the middle part of the Most Formation (*sensu* Shrbený *et al.*, 1994; Fig. 4). The seam has a nearly basin-wide extent and
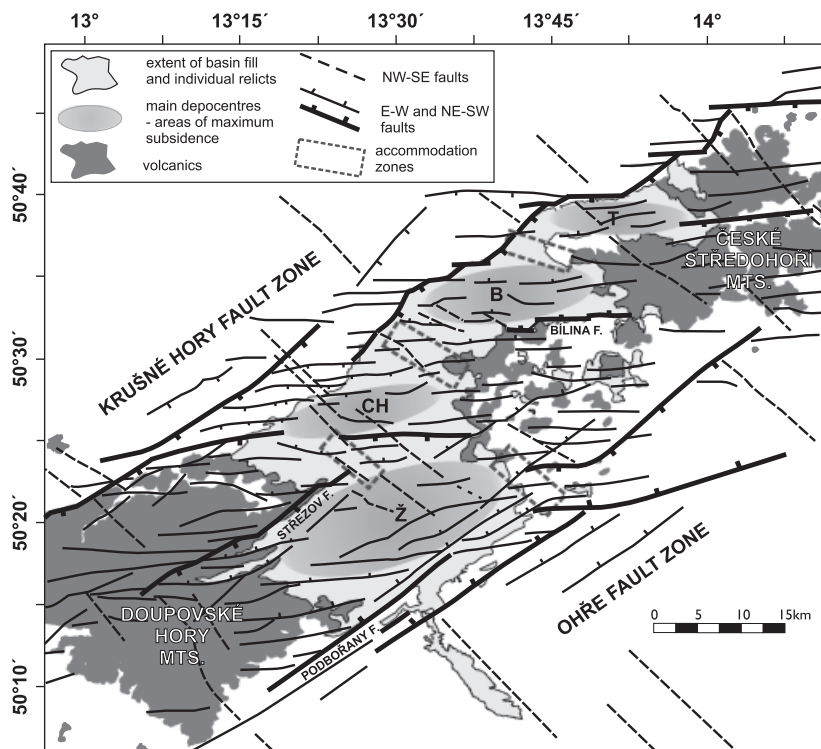
Fig. 13. Structural model of the Most Basin showing individual fault systems and the main depocentres, as interpreted from correlation of gravity maps, isopach maps and digital elevation model (DEM) with brohole-based cross sections and seismic lines. Further comments in text. (B, Bílina Depocentre; CH, Chomutov Depocentre; T, Teplice Depocentre; Ž, Žatec Depocentre).

an average thickness of *ca*. 30 m, reaching locally up to 50 m in response to the underlying topography. The average lignite seam thickness corresponds to a peat accumulation thickness of 180 m or more before loading by clastics, based on the compaction ratio of Hurník (1978). During this interval, two large coarse-grained depositional systems, the Žatec Delta and the Bílina Delta (Dvořák & Mach, 1999; Rajchl & Uličný, 1999, 2005; Rajchl *et al*., 2008), entered the Most Basin from the SE and E, respectively (Fig. 15b), and caused interfingering of the seam with clastics. Some minor clastic systems also developed on the NW margin of the basin during accumulation of the peat (Fig. 15b; e.g. Zelenka & Polický, 1964; Elznic *et al*., 1998).

According to Kovar-Eder *et al*. (2001), the main lignite seam and its clastic equivalents represent a time span of approximately 2 Myr between 20 and 18 Ma (zone MN-3 of European faunal zonation). However, the differential thickness of the main lignite seam, illustrating gradual spreading of the peat swamp from individual depocentres, suggests that the life span of the original peat swamp was probably longer in some places of the basin.

Interval 3 is characterised by a general increase of the depositional area. Deposits of this interval occupy the entire area of the basin, in contrast to the deposits of Interval 2 (Fig. 15b). Clastic equivalents of the seam were probably deposited as far as the volcanic complex of the České Středohoří Mts. during this interval as suggested by isolated erosional relics of fluvial and lacustrine clastics (Fig. 1c; Hurník & Kvaček, 1999). Čadek (1966), Elznic (1970) and Elznic *et al*. (1998) hypothesised that a hydrological outlet draining the Most Basin existed in the area of the present-day Krušné Hory Mountains near Jirkov (Fig. 15). This speculation is based on the extent and orientation of

major fluvial channels of the Žatec Delta (Fig. 15b), and its location coincides with a relay ramp between E–W fault segments at the northwestern end of one of the accommodation zones.

The aggradation of organic material in this remarkable thickness and extent suggests a relatively continuous and accelerated subsidence in the area of the entire basin (cf. Ayers & Kaiser, 1984; Ayers, 1986), also documented by subsidence curves (Fig. 14). This is interpreted as the increase in displacement at major bounding faults at the periphery of the basin (Fig. 15b). Segments of the E–W Bílina Fault actively grew and produced syn-depositional deformation at a time corresponding to the uppermost part of the main lignite seam (Rajchl *et al*., 2008). The Střezov Fault created accommodation for clastics of the Žatec Delta during this time interval (Fig. 3, cross-sections 6, 7), but it is uncertain whether at this time the fault already had the present-day NE–SW strike (possible E–W-trending precursors are indicated by geophysical data, Fig. 5).

The termination of small-displacement intra-basinal faults under or within the main lignite seam, together with the nearly basin-wide extent of the seam, suggests that the small initial depocentres began to merge into larger ones towards the end of Interval 2 and especially during Interval 3 (Fig. 15b).

Interval 4: post-seam clastics (early Miocene–middle Miocene, 18–15 Ma)

Predominantly lacustrine deposits (up to *ca*. 400 m thick) of the upper part of the Most Formation (*sensu* Shrbený *et al*., 1994; Fig. 4) represent the last-known interval of the Most Basin sedimentary evolution. Only carbonaceous deposits of the Lom Seam represent a local interruption of a
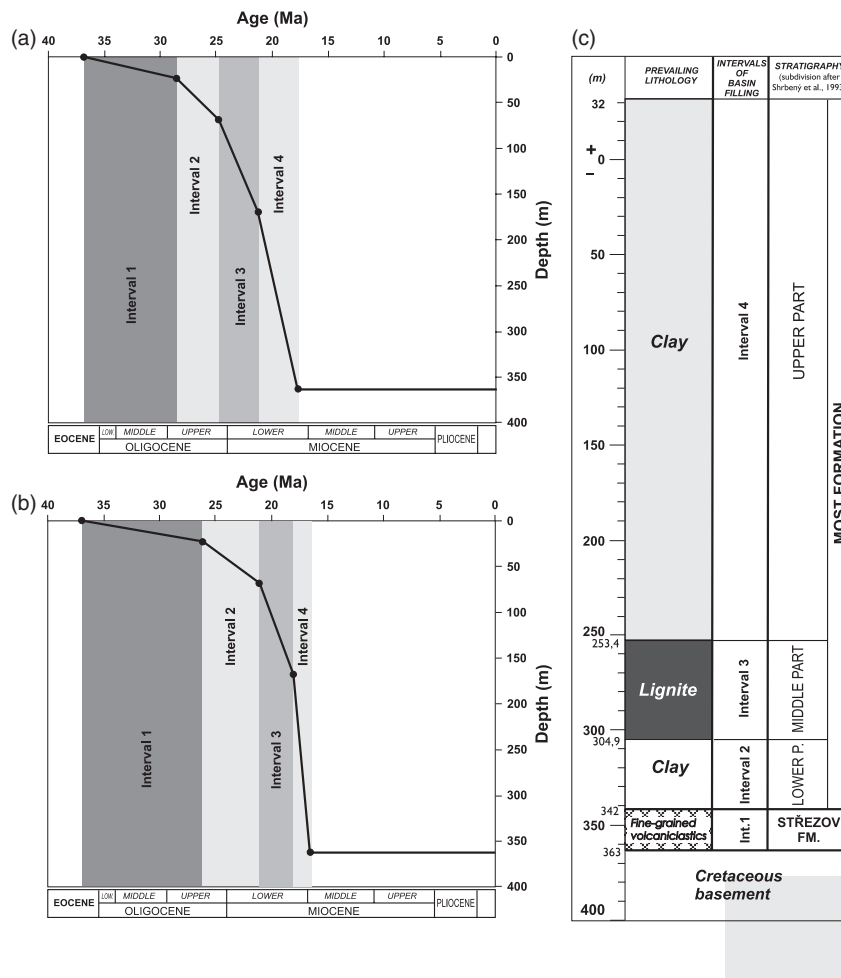
Fig. 14. (a), (b) Decompacted depth-to-basement curve illustrating the subsidence history of the deepest part of the Most Basin. Values for porosity and the 'c' factors of individual sediments were obtained from Sclater & Christie (1980), with the exception of the initial porosity of lignite (peat) of 0.88, after Mach (2003), and the 'c' factor (0.001) derived from the compaction ratio of peat in the Most Basin (6 : 1), as interpreted by Hurník (1972). Dating for the curve in (a) is based on magnetostratigraphic data by Bucha *et al.* (1987). Dating for curve in (b) is based on palaeontological and radiometric data (Bellon *et al.*, 1998; Cajz *et al.*, 1999; Kovar-Eder *et al.*, 2001). Despite differences between the dating methods used and the resulting stratigraphic extent of individual intervals, both curves show very similar results, documenting a gradual increase of the subsidence rate during the Most Basin evolution with an increase towards Interval 4 of basin filling. The subsidence rate estimated for Intervals 1 and 2 (accumulation of the Střezov Formation and the lower part of the Most Formation) is very low, ranging within a few m Myr^{-1}. The subsidence rate during Intervals 3 and 4 (accummulation of the middle and upper parts of the Most Formation) ranged from tens of m Myr^{-1} (during accumulation of peat) to *ca.* 100 m Myr^{-1} (during sedimentation of lacustrine deposits). (c) A composite section created by compilation of lithological data from wells LIH-17 and LB-214, situated in the deepest part of the basin. For the location of the wells, see Fig. 1.

lacustrine sedimentation. The time span of this interval is estimated as either 18–15 Ma (using data of Kovar-Eder *et al.*, 2001) or 21–17.7 Ma based on magnetostratigraphy (Bucha *et al.*, 1987; Malkovský *et al.*, 1989, but note the problems with the magnetostratigraphic methodology mentioned above).

Interval 4 started with a significant increase of the subsidence rate (up to *ca.* 100 m Myr^{-1}; Fig. 14) associated with drowning of the basin-wide swamp and coarse-grained clastic depositional systems (the Bílina and Žatec deltas) by an extensive lake (Figs 3 and 6). The onlap of lacustrine deposits on the body of the Bílina Delta and the surface of the seam (Fig. 6), however, suggests that the process of filling of the accommodation space created was not instantaneous. This is also documented by backstepping of the

youngest deltaic bodies of the Bílina Delta (Rajchl *et al.*, 2008). Because of post-depositional deformation affecting much of the Most Basin, it is difficult to assess the areal extent of the lake at this interval. However, it probably did not reach beyond the present-day margins of the Eger Graben in the Most Basin region (see the discussion below).

The carbonaceous deposits of the Lom Seam (Fig. 3 – cross-sections 4, 9) are interpreted as a swamp forest or mire (Teodoridis & Kvaček, 2006). Together with underlying sand bodies in the central (deepest) part of the Most Basin, it indicates a temporary shallowing of the lacustrine environment. This can be explained by a temporary deceleration of tectonic subsidence and filling of the lake by clastics, or by an increase in the sediment supply rate.
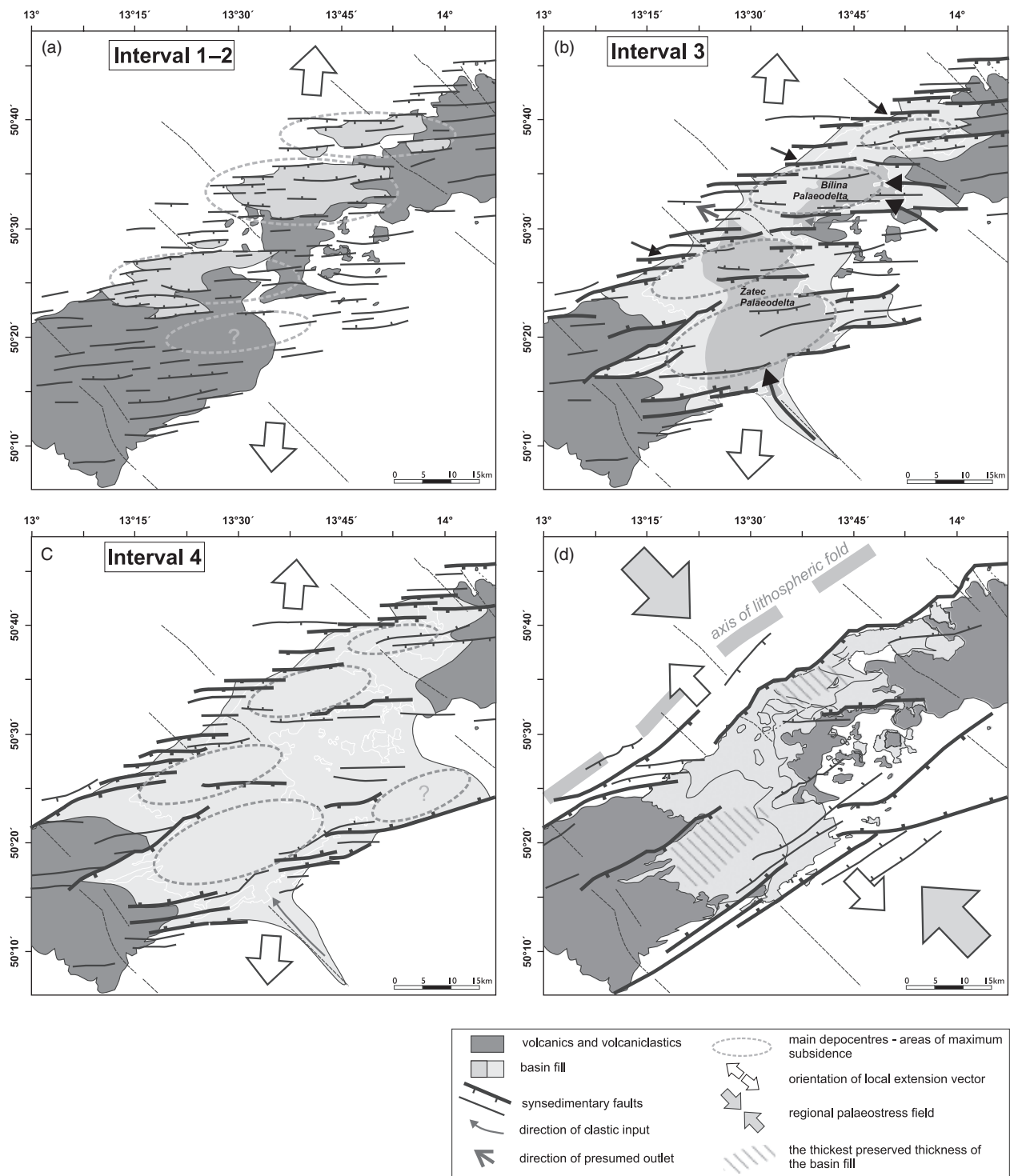
Fig. 15. Cartoons illustrating the interpreted evolution of depocentres and syn- and post-depositional fault systems and the palaeostress interpretations. In (a), the geometry of the earliest syn-depositional fault systems, characterised by E–W- and ENE–WSW-oriented fault segments, is shown together with the position of initial depocentres during Intervals 1 and 2 of the basin evolution. (b) Fault pattern and lateral extent of deposition interpreted for Interval 3, time of peat accumulation. (c) Fault pattern and lateral extent of sedimentation during Interval 4, characterised by formation of a basin-wide lacustrine environment. An increase in the lateral extent of individual depocentres and the depositional area between (a) and (c) documents gradual linkage of the faults and depocentres due to increasing extension. (d) Fault pattern interpreted for postsedimentary orthogonal extension causing destruction of the basin. The extent of clastics shown corresponds to the preserved part of the basin fill.

Post-depositional deformation of the Most Basin

The Eger Graben region underwent a polyphase deformation history, the most recent part of which is associated with the Pliocene to Quaternary uplift of the Krušné Hory Mts. and the related deep incision of some of the rivers in the region, including the Labe (Elbe) River (Váně 1985a; Tyráček, 2001; Tyráček *et al.*, 2004; Ziegler & Dèzes, 2007). Below, we are concerned only with the part of the deformation history that more or less immediately followed the Eger Graben rifting event and is related to normal faulting in the Most Basin area.

A major unconformity, spanning approximately the Mid-Miocene through Early Quaternary, truncates the clastics filling the Most Basin, in a manner similar to other basins of the Eger Graben (Fig. 4). Post-rift, Late Pliocene strata overlying this unconformity in the Cheb Basin indicate that by *ca*. 5 Ma the destruction of the syn-rift basin fills had already been accomplished (Špičáková *et al.*, 2000). According to the study of burial-derived compaction by Hurník (1978), the maximum depth of post-rift erosion of the Most Basin fill is *ca*. 300 m. The lack of direct sedimentary evidence prevents a more accurate dating of the rift-deformation event than between *ca*. 17 and 5 Ma, but shifts in the drainage patterns in the Bohemian Massif (Malkovský, 1979) indicate the onset of uplift in the Eger Graben region in the Middle Miocene.

Along the entire Eger Graben, signs of post-depositional (i.e. post-early Miocene) deformation and erosion are evident. Individual basin fills are relicts preserved in downthrown blocks bounded by NE-trending normal faults, with isolated erosional remnants locally preserved outside the downthrown blocks. This is particularly clear between the Sokolov Basin and the western part of the Most Basin (Špičáková *et al.*, 2000). There, the Krušné Hory and other, parallel fault zones show a marked linearity and great length of individual segments (up to 30 km). In the central and eastern parts of the Most Basin, the NE-trending faults are slightly less prominent, mainly due to the kinked trace of the Krušné Hory Fault, but still very pronounced, and their effects on the basin-fill geometry are very important. Probably the most pronounced tectonic feature is the large-scale flexural deformation of the entire basin fill at its NW margin defined by the Krušné Hory Fault Zone (Fig. 3, e.g. cross–sections 3–5). This was accompanied by hard linkage of some of the earlier E–W faults by NE- to NNE-striking faults, as suggested by DEM data and some of the stratigraphic cross-sections, e.g. sections 2–5 in Fig. 3.

The most detailed insight into this deformation is provided by the seismic reflection profile 68/83 (Figs 3 and 6a) reaching close to the surface trace of the Krušné Hory Fault Zone. The sedimentary package (lignite seam and lacustrine clastics) above the fault zone is fractured by an array of secondary, synthetic normal faults in the folded zone, which splay off the master fault and mostly die out

upward. Immediately above the hinge zone of the flexure, a fan-like array of faults, synthetic and antithetic to the master normal fault, occurs. This array clearly post-dates the lacustrine strata of Interval 4 that show no thinning towards the footwall. The flexure of the entire preserved basin fill is interpreted here as being due to forced folding caused by propagation of a major normal fault in the rigid crystalline basement (see analogue models by Withjack *et al.*, 1990; Hardy & McClay, 1999; Schlische *et al.*, 2002, for similar examples). Contrary to the fault-related folds illustrated by Ford *et al.* (2007, e.g. their Fig. 5), which indicate syn-kinematic deposition throughout the fault evolution, the flexure of the Most Basin fill at the northern edge of profile 68/83 is post-depositional with respect to Interval 4 strata.

Post-depositional faulting along other NE-trending faults, both at the southeastern basin margin and, locally, within the Most Basin, is documented above, as well as the activity of the rift-transverse, NW-trending faults, especially in the Pliocene (Špičáková *et al.*, 2000).

An earlier, potentially still syn-depositional, establishment of NW–SE-directed extension to cause the formation of the NE-trending faults would be implied by the results of Adamovič & Coubal (1999), who infer, on the basis of intrusive body geometries, a period of NW–SE extension between *ca*. 24 and 16 Ma. However, these authors admitted that their conclusion was based on a very small number of dated intrusive bodies.

Evolution of the Most Basin in response to changing palaeostress fields

There is a marked contrast between the syn-depositional role of the E–W-trending fault arrays, typically short and arranged en-echélon along the rift axis, and the mostly post-depositional activity of the rift-parallel, NE-trending faults. Together with the interpreted extension vectors associated with each of the two fault populations, this evokes a scenario of a transition from oblique extension dominating the depositional interval to mainly post-depositional, orthogonal extension, as demonstrated in models by McClay & White (1995), Keep & McClay (1997) and Bonini *et al.* (1997).

Oblique extension: from initiation to fault linkage and depocentre growth (Intervals 1–3)

An oblique-extensional regime dominated the formation of accommodation and relief at E–W-trending fault arrays during most of the basin's recorded lifetime, at least during Intervals 1–3, and probably also Interval 4. (Fig. 15). The angle between the Most Basin axis and the E–W faults (and the axes of depocentres) is *ca*. 30° and most of the meso-scale structural data associated with this fault system indicate NNE (to N)-directed extension (Figs 9a and 10a). This is consistent with data from other parts of the Eger Graben (Peterek *et al.*, 1997; Špičáková *et al.*, 2000;and, partly, Adamovič & Coubal, 1999). This strongly

oblique-extensional setting, with a *ca.* 60° angle between the rift axis and the extension vector, compares well with the analogue models of Tron & Brun (1991), McClay & White (1995), Clifton *et al.* (2000) and McClay *et al.* (2002) as well as with many field examples from oblique-extensional settings (Withjack & Jamison, 1986; Morley *et al.*, 1992; Souriot & Brun, 1992; Brun & Tron, 1993; Bonini *et al.*, 1997; Henry, 1998).

On several observational scales, our data document the successive growth and linkage of the initial dense population of short, oblique-extensional fault segments into several major faults that bordered the depocentres between Intervals 1 and 3 of basin evolution. This is consistent with the scenario of fault growth by gradual linkage of small initial faults, resulting in gradual growth of depocentres and acceleration of subsidence (Cartwright *et al.*, 1995; Gupta *et al.*, 1998; Gawthorpe & Leeder, 2000; McLeod *et al.*, 2000), and contrasts with examples of fault propagation and linkage before significant basin development, shown by (Morley *et al.*, 1999; Morley, 2002). The death of many of the small-displacement faults from the initial stage of basin formation is shown in the seismic sections (Fig. 6) and the propagation of major faults during depocentre development is illustrated e.g. by the syn-depositional fault-propagation folding at the Bílina Fault. The gradual build-up of displacement at linking faults is also reflected in the evolution of subsidence rates. Very slow rates of initial subsidence are analogous to data from the initial phases of rift evolution in the Gulf of Suez or the Jurassic of the North Sea, ranging between < 10 and *ca.* $30 \, \text{m} \, \text{Myr}^{-1}$ and lasting several Myr (Gupta *et al.*, 1998; McLeod *et al.*, 2002).

Advanced fault linkage and subsidence acceleration (Interval 4)

The transition to Interval 4 is marked by an abrupt acceleration of subsidence, accompanied by broadening of the depositional area beyond the preserved limits of the Most Basin fill. The relative increase in the subsidence rate can be explained by the model of Gupta *et al.* (1998) invoking strain localisation on linked fault arrays and not necessitating an increased strain rate or a change in the extension vector orientation. The fact that the increase in subsidence rates occurred simultaneously in two other basins of the Eger Graben, recorded by onset of the lacustrine Cypris Formation (Špičáková *et al.*, 2000), however, suggests that some overriding, regional control may have acted in this case. This might have been an increase in the strain rate, possibly induced by a change of the stress field. With regard to indices that some of the NE–SW faults may have been active syn-depositionally, we discuss below whether the increase in the subsidence rate during Interval 4 could be related to the beginning of a change in the palaeostress field that later led to the post-depositional deformation and termination of the rift regime of the entire Eger Graben. Based on the available data, however, the preferred interpretation is that Interval 4 represents an advanced stage of fault linkage that caused basin-wide deposition in depocentres deepened along a reduced number of major faults.

Orthogonal extension: post-rift deformation and erosion of the basin fill

The post-depositional deformation described above implies a local NW–SE-oriented extension, orthogonal with respect to the rift axis, and resulting in linear fault segments (McClay & White, 1995; McClay *et al.*, 2002). In addition to the large-scale geometry of the NE–SW-trending faults, the orthogonal extension is supported by some of the mesoscopic structural data and the observed linkage of some of the E–W fault segments in the Krušné Hory Fault Zone by NE- to NNE-trending faults. A change in the extension vector orientation, from the NNE–SSW, oblique extension, to the roughly NW–SE direction of post-sedimentary orthogonal extension, was earlier interpreted by Rajchl & Uličný (2000) and Špičáková *et al.* (2000). Notably, the post-depositional normal faulting occurred in an area narrower than the region of oblique extension, generally between the Krušné Hory FZ and the rift axis. The only exception is the Žatec depocentre downthrown post-depositionally. This part of the Eger Graben evolution is referred to as post-rift because it involves a partial inversion and significant erosion of the basin fill, significant reduction of volcanism and the associated normal faulting is interpreted below as a consequence of regional lithospheric folding (e.g. Dèzes *et al.*, 2004).

DISCUSSION

Evidence for the transition from the oblique to the orthogonal extension mode

Rift-marginal faults in oblique-extensional regimes can propagate and link to form nearly rift-parallel faults under increasing extensional strain either due to a change in the extension direction or under unchanged stress orientation (Tron & Brun, 1991; McClay & White, 1995; McClay *et al.*, 2002). It is therefore important to review the combination of evidence leading to the above interpretation of a change in extension vectors in the Most Basin. A number of features in the Most Basin structural pattern are analogous to those observed by Bonini *et al.* (1997) for a change from oblique to orthogonal extension, with the angle between the extensional vectors moderately exceeding 45°, and by Keep & McClay (1997) for similar situations:

(i) numerous oblique faults displaying an en echélon geometry developed in the central part of the rifted domains during oblique extension;

(ii) almost no previous oblique faults continued to grow during the orthogonal extension, and new normal faults developed parallel to the rift axis, as illustrated by the formation of the Ohře Fault Zone and NE–SW-trending segments of the Krušné Hory Fault Zone breaching former relay ramps; and

(iii) a master fault developed during orthogonal extension, in a zone previously weakened by small oblique faults,

resulting in a wavy surface trace, accompanied by kinks, salients and embayments that mark the locations of linkage – this is analogous to the kinked trace of the Krušné Hory Fault, and typical of situations with a high degree of initial extension obliquity.

Overall, the formation of prominent rift-parallel marginal faults in an oblique-extensional regime was observed to result from high volumes of extension (up to 50% in models of McClay *et al*., 2002), which is not the case for the Most Basin: total stretching estimated across the Most Basin is *ca*. 8%, based on the throw and heave distances measured at pre-rift markers at the base of the basin fill. The length and straightness of some of the NE–SW fault segments (especially the Ohře Fault Zone) support the interpretation of their formation by orthogonal (NW–SE) extension.

Unlike analogue models, field examples are strongly influenced by the basement structure. The differences in the geometry of the main bounding fault zones of the Most Basin (kinked Krušné Hory FZ vs. mainly straight and parallel Ohře FZ) were probably influenced by basement fabrics that supported or partially overprinted the effect of extension orientation. The kinks in the Krušné Hory FZ (of 35–50° angle between individual segments) are developed in the Saxothuringian crystalline basement underlying this part of the rift area that is characterised by E–W fabrics (Mlčoch, 1994). In contrast, the southeastern part of the Most Basin is underlain by an Upper Palaeozoic graben of the Kladno-Rakovník Basin (Pešek, 1994) defined by NE–SW faults. Although this inherited fabric might theoretically have helped to direct the faults forming during the oblique-extensional phase into parallelism with the Eger Graben axis, the existence of E–W faults developed in the same substratum (e.g. the fault zone followed by Ohře River) indicates that the two stress fields led to the formation of directionally disctinct fault populations independent of the basement structure. We conclude that the differences in the basement fabric between the opposite sides of the basin probably did not lead to development of NE–SW faults in the oblique-extensional regime, but caused a slightly different orientation of the NE–SW fault segments on each side.

Timing of post-depositional faulting

One of the keys to understanding the stress field evolution during the latest intervals of deposition in the basin is the relationship of the Krušné Hory Fault Zone with the depocentres and intrabasinal faults. The composite nature of the Krušné Hory FZ, with parts of E–W faults hard-linked across breached relay ramps or even with some relay ramps only tilted without breaching, was a source of major disputes about the role of the Krušné Hory FZ in the origin of the Most Basin in earlier local literature (Malkovský, 1966, 1979; Hurník & Havlena, 1984; Kopecký *et al*., 1985; Marek, 1985; Váně, 1985a).

With regard to the relationship between the boundary faults and the intra-basinal fault framework, some analogies may be found between the Most Basin and the Rukwa Rift. The latter, interpreted by Ring *et al*. (1992) initially as an oblique rift (see also McClay & White, 1995), later deformed in a strike–slip regime. Although different in kinematics and probably of a much longer history than the Krušné Hory FZ, the Lupa Fault of the Rukwa Rift is also a major border fault overprinting part of the earlier depocentres (cf. Fig. 10 in Morley, 2002). Its kinked shape in the map view indicates origin by linkage of many smaller segments, but, unlike the Krušné Hory FZ, the Lupa Fault has a significant record of syn-depositional activity. In case of the Krušné Hory FZ, the post-depositional activity is clear due to basin-fill deformation, but it is questionable to which extent its formation (by coalescence of earlier oblique faults) may have influenced the basin filling during Interval 4.

Onlap of the main lignite seam on the Cretaceous substratum occurs near the northern edge of seismic line 68/83, beyond 6 km, and thinning of lacustrine deposits immediately above the seam is observed between 5 and 6 km (Fig. 6a). This is interpreted as a record of a relay ramp evolution between two propagating, syn-depositional fault segments. However, the younger part of the lacustrine stratal package of Interval 4 shows no thinning towards the basin margin, and is affected by a clearly post-depositional deformation related to fault propagation. Most probably, the E–W fault segments bounding this relay ramp became linked before the onset of Interval 4, or their displacement was transferred to another fault in a more outward position. The exact timing of the post-depositional deformation shown in Fig. 6a, however, remains unclear – it may have occurred immediately after the Interval 4 termination or later, during the Miocene or even Pliocene.

Another example of a syn-depositional relay ramp in the vicinity of the Krušné Hory FZ is the locality Hradiště (Fig. 7) where a relict of fluvial sands is preserved beyond the trace of the Krušné Hory FZ. A small fluvial feeder system transporting clastics southward most probably sourced a prograding deltaic sand wedge high in the Most Formation lacustrine deposits (Váně, 1985a) – during Interval 4. Because the Hradiště sandstones rest on the crystalline basement, the ramp must have been uplifted and probably tilted before or during this depositional episode. This could have occurred during propagation of an E–W fault segment late during Interval 3 or 4. The Hradiště ramp and adjacent small relay ramps to its SW were never breached. However, a straight, NE–SW-trending fault trace occurs further NW, in the basin periphery, as a continuation of the Krušné Hory FZ. This fault is most probably post-depositional because its syn-depositional activity during Interval 4 would have caused wholesale hangingwall subsidence of the adjacent E–W segments and the Hradiště ramp.

The above lines of evidence lend further support to the interpretation of a post-depositional change in the exten-

sion vector, from NNE–SSW to NW–SE, that led to post-depositional faulting and related basin-fill deformation in the Most Basin region and elsewhere in the Eger Graben. Importantly, the post-depositional normal faulting was concentrated in a zone narrower than the syn-depositional width of the Most Basin, along the Krušné Hory FZ and, partly, the Střezov Fault, showing a different structural style than the syn-depositional fault growth that caused broadening of the depositional area during Interval 4. Yet another indirect support for the post-depositional change in the extension regime comes from the consideration that with an unchanged stress field, continued linkage of normal faults would have led to a further increase in the subsidence rates in the depocentres, rather than to their uplift and erosion (cf. Gawthorpe & Leeder, 2000).

Implications for geodynamic causes of Eger Graben and ECRIS extension

With regard to the palaeostress history of the entire ECRIS and the geodynamic causes of its evolution, the data from the Most Basin in the central part of the Eger Graben are very important. All the data presented here show that *ca*. 18 Myr of basin-filling history were governed by regional N–S to NNE–SSW extension, similar to other parts of the Eger Graben. This rules out the idea of Bourgeois *et al.* (2007) that the ECRIS formed a left-lateral wrench zone fringing the Alpine front from the Mediterranean to the Bohemian Massif, with the Eger Graben opening as a purely strike–slip structure.

This Oligocene–early Miocene local stress field of the Most Basin, however, was different from that of other parts of the ECRIS, dominated by E–W to WNW–ESE extension in the western and central parts (e.g. Michon *et al.*, 2003). It is not easy to reconcile the N–S, and later NW–SE extension, interpreted here for the Eger Graben, with a coeval continental palaeostress field characterised by N–S-oriented compression (e.g. Bergerat, 1987; Dèzes *et al.*, 2004). One possible explanation for this autonomous palaeostress field of the Eger Graben is the hypothesis of Michon *et al.* (2003) and Michon & Merle (2005) invoking a slab-pull model, with downward gravitational stresses induced by formation of the Alpine lithospheric root, causing formation of ECRIS rifts essentially by passive rifting. In this model, the direction of foreland extension is approximately perpendicular to the lithospheric root and parallel to the direction of compression induced by Africa–Europe collision.

However, the entire Eger Graben, especially its central part including the Most Basin, is characterised by large volumes of volcanics that pre-dated the main phase of clastic sedimentation. This may support the idea of thermal-driven doming suggested by Dèzes *et al.* (2004) for the Eger Graben, although in general they explained the initiation of the ECRIS mainly by the build-up of syn-collisional compressional intraplate stresses caused by collision of Africa and Europe. The mantle-plume origin of European

Cenozoic rifts, commonly invoked in the 1990s (Wilson & Downes, 1992; Granet *et al.*, 1995, among others), has been deemphasised in the recent literature; Wilson & Downes (2006) conclude that partial melting of the mantle was induced by adiabatic decompression of the asthenosphere, triggered by mantle upwelling, and envisage small-scale, plume-like diapirs possibly upwelling from *ca*. 400 km depth. The evolution of the Most Basin suggests that weak extension in response to thermal doming should be considered in case of the opening of the Eger Graben case, regardless of the origin of the melts. The relief and stratigraphic record around the Eger Graben have been considerably altered by post-Miocene erosion, and thus it is difficult to verify the possibility of a thermal dome evolution by palaeodrainage reconstruction. However, during Interval 2 the Most Basin filling was dominated by redeposition of volcanic material, and in Interval 3, peat accumulation dominated over clastics for a long time in most of the basin, except the Žatec Delta region, where a clastic pathway followed a transverse basement fault zone. This indicates that there was little significant regional clastic input into the centre of the Eger Graben, until *ca*. 18 Ma, which may be indirect support for regional doming.

The later, NW–SE oriented, extension related to the formation of the Krušné Hory FZ and other present-day bounding faults of the Eger Graben represents a local palaeostress field. Its orientation contrasts with the Miocene–Pliocene build-up of NW–SE compression that dominates Central Europe today (Cloetingh & Kooi, 1992; Ziegler & Dèzes, 2007). The formation of a local extensional domain in an overall compressional stress field, however, lends support to the idea of Miocene-age lithospheric folding as proposed by Dèzes *et al.* (2004). We interpret the post-depositional normal faulting in the Most Basin as along-crest extension during the growth of a broadly SW–NE-trending, lithosphere-scale, anticlinal feature that extends from the Massif Central via the Burgundy transfer zone towards the Bohemian Massif (Fig. 1). Dèzes *et al.* (2004) and Bourgeois *et al.* (2007) dated the onset of lithospheric folding in the previously thermally weakened ECRIS domain as 18 or 17 Ma, respectively. This time roughly corresponds to the termination of the Most Basin filling (according to palaeomagnetic dating, Bucha *et al.*, 1987). Similar to other ECRIS basins affected by the lithospheric folding, the Most Basin is tilted and partly eroded (cf. Bourgeois *et al.*, 2007), with the fault-propagation fold shown in Fig. 6a being perhaps the most graphic evidence of basin deformation in this phase of ECRIS evolution. The fact that the Eger Graben is located on the southeastern shoulder of the interpreted lithospheric fold structure, parallel to its axis (Fig. 1), but not exactly in a crestal position, can be explained by the rheological heterogeneity of the basement.

After the Eger Graben syn-rift sedimentation was terminated by the lithospheric folding, the Pliocene–Quaternary sedimentation and volcanism in the region were confined mainly to NW-trending fault zones cross-cutting the graben and activated as sinistral strike–slip zones (e.g. Špičáková *et al.*, 2000). The interaction of these

zones with individual segments of the ancient E–W fault system could have caused the formation of small pull-apart structures filled by alluvial clastics (Fig. 2). The interaction between the Mid-Miocene to Recent compressional stress field, lithospheric buckling, crustal heterogeneity and the resulting patterns of uplift, and erosion/sedimentation in the entire Eger Graben region remains poorly understood and represents an important challenge for future research.

SUMMARY

The Most Basin provides a good illustration of initiation, gradual growth and linkage of normal fault arrays in a strongly oblique-extensional situation, overprinted by a post-depositional phase of orthogonal extension that caused significant deformation of the basin fill. The fault geometries compare well with published analogue models of rifts undergoing oblique to orthogonal extension, although the different basement fabrics in the crustal blocks separated by the rift axis influenced the local expression of some fault populations.

The preserved stratigraphic record shows that the basin evolution stopped shortly after the transition from the initial rifting stage to a more mature stage with subsidence accelerated along major depocentre-bounding faults. The post-depositional faulting and formation of an adjacent uplift resulted from a localised extensional collapse along the crest of a growing lithospheric fold. The total estimated stretching of *ca*. 8% is in accordance with the very slow subsidence rates over most of the recorded basin history.

The timing of the basin filling as well as its destruction correlate well with events occurring elsewhere in the Eger Graben, and also with the timing of onset of rifting (*ca*. 37 Ma) and the presumed lithospheric folding (*ca*. 18 Ma) in the entire ECRIS. The indigenous stress field, abundant volcanism and relative clastic starvation during the depositional Intervals 1–3 suggest that a possibility of thermal doming as the cause of rifting initiation should not be excluded in further studies of the Eger Graben.

REFERENCES

Adamovič, J. & Coubal, M. (1999) Intrusive geometries and Cenozoic stress history of the northern part of the Bohemian Massif. *Geolines*, **9**, 5–14.

Aldrich, M.J. Jr., Chapin, C.E. & Laughlin, A.W. (1986) Stress history and tectonic development of the Rio Grande rift, New Mexico. *J. Geophys. Res.*, **91**(B6), 6199–6211.

Arthaud, F. & Matte, P. (1977) Late Paleozoic strike–slip faulting in southern Europe and northern Africa: result of a right-lateral shear zone between the Appalachians and the Urals. *GSA Bull.*, **88**, 1305–1320.

Ayers, W.B. (1986) Lacustrine-interdeltaic coal in Forth Union Formation (Paleocene), Powder River Basin, Wyoming and Montana. *AAPG Bull.*, **70**, 1651–1673.

Ayers, W.B. & Kaiser, W.R. (1984) Lacustrine-interdeltaic coal in Forth Union Formation (Paleocene). *AAPG Bull.*, **68**, 931–931.

Babuška, V. & Plomerová, J. (2006) European mantle lithosphere assembled from rigin microplates with inherited seismic anisotropy. *Phys. Earth Planet. Inter.*, **158**, 264–280.

Bellon, H., Bůžek, Č., Gaudant, J., Kvaček, Z. & Walther, H. (1998) The České středohoří magmatic complex in Northern Bohemia ^{40}K–^{40}Ar ages for volcanism and biostratigraphy of the Cenozoic freshwater formations. *Newslett. Dtratigr.*, **36**, 77–103.

Bergerat, F. (1987) Strss-fields in the European platform at the time of Africa–Eurasia collision. *Tectonics*, **6**, 99–132.

Bonini, M., Souriot, T., Boccaletti, M. & Brun, J.P. (1997) Successive orthogonal and oblique extension episodes in a rift zone: laborytory experiments with application to the Ethiopian Rift. *Tectonics*, **16**, 347–362.

Bourgeois, O., Ford, M., Diraison, M., Le Carlier De Veslud, C., Gerbault, M., Pik, R., Ruby, N. & Bonnet, S. (2007) Separation of rifting and lithospheric folding signatures in the NW-Alpine foreland. *Int. J. Earth. Sci. (Geol. Rundsch.)*, **96**, 1003–1031.

Brun, J.P. & Tron, V. (1993) Development of the North Viking Graben – inferences from laboratory modelling. *Sediment. Geol.*, **86**, 31–51.

Brus, Z. & Hurník, S. (1987) Longitudinal fault "Eliška" and its mineralization in the opencast Obránců míru Mine in the North Bohemian brown-coal basin (in Czech with English summary). *Čas. Min. Geol.*, **32**, 133–142.

Bucha, V., Elznic, A., Horáček, J., Malkovský, M. & Pazderová, J. (1987) Paleomagnetic timing of the Tertiary of the North Bohemian Brown-Coal-Basin. *Věst. Ústř. Úst. Geol.*, **62**(2), 83–95.

Čadek, J. (1966) Nové poznatky o paleogeografii chomutovsko-mostecko-teplické pánve (na základě studia těžkých minerálů). *Sbor. Geol. Věd, Geol.*, **11**, 77–114.

Cajz, V. (2000) Proposal of lithostratigraphy for the České středohoří Mts. volcanics. *Bull. Czech Geol. Surv.*, **75**, 7–16.

Cajz, V. (2001) Vmístění žilného roje v okolí vulkanického centra Českého středohoří. PhD Thesis, Institute of Geology, Academy of Sciences of the Czech Republic. 111 pp.

Cajz, V., Vokurka, K., Balogh, K., Lang, M. & Ulrych, J. (1999) The České středohoří Mts. volkanistratigraphy and geochemistry. *Geolines*, **9**, 21–28.

Cartwright, J.A., Trudgill, B.D. & Mansfield, C.S. (1995) Fault growth by segment linkage: an explanation for scatter in maximum displacement and trace length data from the Canyonlands Grabens of SE Utah. *J. Struct. Geol.*, **17**, 1319–1326.

Clifton, A.E., Schlische, .R.W., Withjack, M.O. & Ackermann, R.V. (2000) Influence of rift obliquity on fault-population systematics: results of experimental clay models. *J. Struct. Geol.*, **22**, 1491–1509.

Cloetingh, S. & Kooi, H. (1992) Tectonics and global change – inferences from Late Cenozoic subsidence and uplift patterns in the Atlantic mediterranean region. *Terra Nova*, **4**, 340–350.

Cowie, P.A., Gupta, S. & Dawers, N.H. (2000) Implications of fault array evolution for synrift depocentre development: insights from a numerical fault growth model. *Basin Res.*, **12**, 241–261.

Dèzes, P., Schmid, S.M. & Ziegler, P.A. (2004) Evolution of the European Cenozoic Rift System: interaction of the Alpine and Pyrenean orogens with their foreland lithosphere. *Tectonophysics*, **389**, 1–33.

Dèzes, P., Schmid, S.M. & Ziegler, P.A. (2005) Reply to comments by L. Michon and O. Merle on "Evolution of the European Cenozoic Rift System: interaction of the Alpine and Pyrenean orogens with their foreland lithosphere" by P. Dèzes, S.M. Schmid and P.A. Ziegler, Tectonophysics 389 (2004) 1–33. *Tectonophysics*, **401**(3–4), 257–262.

Domácí, L. (1977) Litostratigrafie třetihorních sedimentů v hnědouhelné severočeské pánvi. *Acta Univ. Car. – Geol.*, **1**, 75–80.

Doré, A.G., Lundin, E.R., Fichler, C. & Olesen, O. (1997) Patterns of basement structure and reactivation along the NE Atlantic margin. *J. Geol. Soc.*, **154**, 85–92.

Dvořák, Z. & Mach, K. (1999) Deltaic deposits in the North-Bohemian Brown Coal Basin and their documentation in the Bílina opencast mine. *Acta Univ. Car. – Geol.*, **43**, 633–641.

Elznic, A. (1963) Severozápadní omezení Chomutovsko-mostecko-teplické pánve. *Věstník ÚÚG*, **38**, 245–253.

Elznic, A. (1970) Litofaciální vývoj a paleogeografie terciéru na Mostecku, Teplicku a Ústecku. *Zpr. Stud. Obl. Vlastivěd. Muz. Přír. Vědy*, 3–13. Teplice.

Elznic, A., Čadková, Z. & Dušek, P. (1998) Paleogeografie terciérních sedimentů severočeské pánve. *Sbor. geol. Věd. Geol.*, **48**, 19–46.

Fejfar, O. & Kvaček, Z. (1993) Excursion No. 3. Tertiary basins in Northwest Bohemia. Paleontol. Ges. 63. Jahrestagung, Prag. Charles Univ. Prague.

Ford, M., Le Carlier De Veslud, C. & Bourgeois, O. (2007) Kinematic and geometric analysis of fault-related folds in a rift setting: The Dannemarie basin, Upper Rhine Graben, France. *J. Struct. Geol.*, **29**, 1811–1830.

Gapais, D., Cobbold, P.R., Bourgeois, O. & De Urreiztieta, M. (2000) Tectonic significance of fault-slip data. *J. Struct. Geol.*, **22**, 881–888.

Gawthorpe, R.L. & Leeder, M.R. (2000) Tectono-sedimentary evolution of active extensional basins. *Basin Res.*, **12**, 195–218.

Granet, M., Wilson, M. & Achauer, U. (1995) Imaging a mantle plume beneath the French Massif Central. *Earth Planet. Sci. Lett.*, **136**(3–4), 281–296.

Gupta, S., Cowie, P.A., Dawers, N.H. & Underhill, J.R. (1998) A mechanism to explain rift-basin subsidence and stratigraphic patterns through fault-array evolution. *Geology*, **26**, 595–598.

Gupta, S., Underhill, J.R., Sharp, I.R. & Gawthorpe, R.L. (1999) Role of fault interactions in controlling synrift sediment dispersal patterns: Miocene, Abu Alaqua Group, Suez Rift, Sinai, Egypt. *Basin Res.*, **11**, 167–189.

Hardy, S. & McClay, K. (1999) Kinematic modelling of extensional fault-propagation folding. *J. Struct. Geol.*, **21**, 695–702.

Henry, C.D. (1998) Basement-controlled transfer zones in an area of low-magnitude extension, eastern Basin and Range province, Trans-Pecos Texas. In: *Accommodation Zones and Transfer Zones: The Regional Segmentation of the Basin and Range Province* (Ed. by J.E. Faulds & J.J. Stewart), Geol. Soc. Am. Spec. Pap., **323**, 75–89.

Hradecký, P. (1977) K tektonickému a sedimentačnímu vývoji v centrálním úseku pooháreckého zlomového pásma. *Věst. Úst. Ústř. Geol.*, **52**, 285–292.

Hurník, S. (1972) Koeficient sednutí některých sedimentů v Severočeské hnědouhelné pánvi. *Čas. Min. Geol.*, **17**, 365–371.

Hurník, S. (1978) Rekonstrukce mocnosti nadložních souvrství v severočeské hnědouhelné pánvi (miocén). *Čas. Min. Geol.*, **23**, 265–275.

Hurník, S. & Havlena, V. (1984) Podkrušnohorské hnědouhelné pánve a Krušné hory jako součásti neotektonické velevrásové struktury. *Čas. Min. Geol.*, **29**, 55–67.

Hurník, S. & Kvaček, Z. (1999) Satellite basin of Skyřice near Most and its fossil flora (Miocene). *Acta Univ. Carol. – Geol.*, **43**, 643–656.

Illies, J.H. & Greiner, G. (1978) Rhine Graben and alpine system. *Geol. Soc. Am. Bull.*, **89**, 770–782.

Jihlavec, F. & Novák, J. (1986) Reflexně seismická měření v severočeské pánvi. *Geologický průzkum*, **5**/**1986**, 136–138.

Jindřich, V. (1971) New views in tectonic significance of platform sediments in the Bohemian Massif, Czechoslovakia. *Geol. Soc. Am. Bull.*, **82**, 763–768.

Kasiñski, J.R. (2000) *Geological Atlas of the Tertiary Lignite-Bearing Association in the Polish Part of the Zittau Basin*. Pañstwowy Institut Geologiczny, Warszawa.

Keep, M. & McClay, K.R. (1997) Analog modelling of multi-phase rift systems. *Tectonophysics*, **273**, 239–270.

Konopásek, J., Schulmann, K. & Lexa, O. (2001) Structural evolution of the central part of the Krusne hory (Erzgebirge) Mountains in the Czech Republic – evidence for changing stress regime during Variscan compression. *J. Struct. Geol.*, **23**(9), 1373–1392.

Kopecký, L. (1978) Neoidic taphrogenic evolution and young alkaline volcanism of the Bohemian Massif. *Sbor. geol Věd, Geol.*, **31**, 91–108.

Kopecký, L., Květ, R. & Marek, J. (1985) Kotázce existence krušnohorského zlomu. *Geologický průzkum*, **6**, 164–168.

Kossmat, F. (1927) *Übersicht der Geologie von Sachsen*. G.A. Kaufmann, Leipzig.

Kovar-Eder, J., Kvaček, Z. & Meller, B. (2001) Comparing Early to Middle Miocene floras and probable vegetation types of Oberdorf N Voitsberg (Austria), Bohemia (Czech Republic), and Wackersdorf (Germany). *Rev. Paleobot. Palynol.*, **114**, 83–125.

LE TURDU, C., RICHERT, J.P., XAVIER, J.P., RENAUT, R.W., TIERCELIN, J.J., ROLET, J., LEZZAR, K.E. & COUSSEMENT, C. (1999) Influence of preexisting oblique discontinuities on the geometry and evolution of extensional fault pattern: evidence from the Kenya rift using SPOT imager. In: *Geoscience of Rift Systems – Evolution of East Africa* (Ed. by C.K. Morley), *AAPG Stud. Geol.*, **44**, 173–191.

MACH, K. (2003) Anomální stavba hlavní hnědouhelné sloje v prostoru miocenní bílinské delty a její geneze. PhD thesis, Charles University, Prague.

MALKOVSKÝ, M. (1966) Strukturní a tektonické poměry křídy a terciéru při východní části Krušných hor. *Sbor. geol. Věd, Geol.*, **11**, 135–152.

MALKOVSKÝ, M. (1979) Tektogeneze platformního pokryvu Českého masívu. *Knih. ÚÚG*, **53**. Praha.

MALKOVSKÝ, M. (1987) The Mesozoic and Tertiary basins of the Bohemian Massif and their evolution. *Tectonophysics*, **137**, 31–42.

MALKOVSKÝ, M., et al. (1985) *Geologie severočeské hnědouhelné pánve a jejího okolí.* ÚÚG, Academia, Praha.

MALKOVSKÝ, M., BUCHA, V. & HORÁČEK, J. (1989) Rychlost sedimentace terciéru v mostecké části severočeské hnědouhelné pánve. *Geologický Průzkum*, **1**, 2–5.

MAREK, J. (1985) Existuje krušnohorský zlom? *Čas. Min. Geol.*, **30**, 39–51.

MATTE, P., MALUSKI, H., RAJLICH, P. & FRANKE, W. (1990) Terrane boundaries in the Bohemian Massif – result of large-scale Variscan Shearing. *Tectonophysics*, **177**(1–3), 151–170.

MCCARTHY, T.S., ELLERY, W.N. & STANISTREET, I.G. (1992) Avulsion mechanisms on the Okavango fan, Botswana: the control of a fluvial system by vegetation. *Sedimentology*, **39**, 779–795.

MCCLAY, K.R., DOOLEY, T., WHITEHOUSE, O. & MILLS, M. (2002) 4-D evolution of rift systems: isights from scaled physical models. *AAPG Bull.*, **86**, 935–359.

MCCLAY, K.R. & WHITE, M.J. (1995) Analogue modelling of orthogonal and oblique rifting. *Mar. Petrol. Geol.*, **12**, 137–151.

MCLEOD, A.E., DAWERS, N.H. & UNDERHILL, J.R. (2000) The propagation and linkage of normal faults: insights from the Strathspey-Brent-Statfjord fault array, northern North Sea. *Basin Res.*, **12**(3–4), 263–284.

MICHON, L. & MERLE, O. (2005) Discussion on "Evolution of the European Cenozoic Rift System: interaction of the Alpine and Pyrenean orogens with their foreland lithosphere" by P. Dèzes, S.M. Schmid and P.A. Ziegler, Tectonophysics 389 (2004) 1–33. *Tectonophysics*, **401**(3–4), 251–256.

MICHON, L., VAN BALEN, R.T., MERLE, O. & PAGNIER, H. (2003) The Cenozoic evolution of the Roer valley rift system integrated at a European scale. *Tectonophysics*, **367**, 101–126.

MLČOCH, B. (1994) The geological structure of the Crystalline basement below the North Bohemian brown coal basin. *KTB Rep.*, **94**(3), 39–46.

MLČOCH, B. & MARTÍNEK, K. (2002) Tectonosedimentary evolution of NW Bohemia based on the digital elevation model of crystalline basement and upper paleozoic strata: preliminary results. *Geolines*, **14**, 67–68.

MORLEY, C.K. (1999) Influence of preexisting fabrics on rift structure. In: *Geoscience of Rift Systems – Evolution of East Africa* (Ed. by C.K. Morley), *AAPG Stud. Geol.*, **44**, 151–160.

MORLEY, C.K. (2002) Tectonic settings of continental extensional provinces and their impact on sedimentation and hydrocarbon prospectivity. In: *Sedimentation in Continental Rifts* (Ed. by R.W. Renaut & G.M. Ashley), *SEPM Spec. Publ.*, **73**, 25–55.

MORLEY, C.K., CUNNINGHAM, S.M., HARPER, R.M. & WESCOTT, W.A. (1992) Geology and geophysics of the Rukwa Rift, East Africa. *Tectonics*, **11**, 69–81.

MORLEY, C.K., CUNNINGHAM, S.M., WESCOTT, W.A. & HARPER, R.M. (1999) Geology and geophysics of the Rukwa rift. In: *Geoscience of Rift Systems – Evolution of East Africa* (Ed. by C.K. Morley), *AAPG Stud. Geol.*, **44**, 91–110.

MORTIMER, E., GUPTA, S. & COWIE, P. (2005) Clinoform nucleation and growth in coarse-grained deltas, Loreto basin, Baja California Sur, Mexico: a response to episodic accelerations in fault displacement. *Basin Res.*, **17**, 337–359.

PEACOCK, D.C.P., KNIPE, R.J. & SANDERSON, D.J. (2000) Glossary of normal faults. *J. Struct. Geol.*, **22**, 291–305.

PEACOCK, D.C.P. & SANDERSON, D.J. (1994) Geometry and development of relay ramps in normal fault systems. *AAPG Bull.*, **78**, 147–165.

PERESSON, H. (1992) Computer aided kinematic analysis of fault sets. *Mitt. Ges. Geol. Bergbaustud.*, **38**, 107–119, Vienna.

PEŠEK, J. (1994) *Carboniferous of Central and Western Bohemia (Czech Republic).* Czech Geological Survey, Prague.

PETEREK, A., RAUCHE, H., SCHRÖDER, B., FRANZKE, H.J., BANKWITZ, A. & BANKWITZ, E. (1997) The late- and post-Variscan tectonic evolution of the Western Border fault zone of the Bohemian massif (WBZ). *Geol. Rundsch.*, **86**, 191–202.

RAJCHL, M. (2006) Tectonosedimentary evolution and fluvio-deltaic systems of the Most Basin (Tertiary, Eger Graben, Czech Republic). PhD thesis, Charles University, Prague.

RAJCHL, M. & ULIČNÝ, D. (1999) Sedimentární model bílinské delty (The depositional model of the Bílina delta). *Zpravodaj Hnědé uhlí*, 3/99, 15–42 (in Czech with English summary).

RAJCHL, M. & ULIČNÝ, D. (2000) Evolution of basin-fill geometries in the Most Basin: implications for the tectonosedimentary history of the Ohře Rift (Eger Graben), North Bohemia. Proceedings of the 5th meeting of the Czech Tectonic Studies Group. *GeoLines*, **10**, 62–63.

RAJCHL, M. & ULIČNÝ, D. (2005) Depositional record of an avulsive fluvial system controlled by peat compaction (Neogene, Most Basin, Czech Republic). *Sedimentology*, **52**, 601–625.

RAJCHL, M., ULIČNÝ, D. & HUBATKA, F. (2003a) Syn- and post-sedimentary tectonics of the Most Basin (Ohře Rift, Czech Republic); insights from reflection-seismic data. Proceedings of the 8th Meeting of the Czech tectonic Studies Group. *GeoLines*, **16**, 86.

RAJCHL, M., ULIČNÝ, D. & MACH, K. (2008) Interplay between tectonics and compaction in a rift-margin, lacustrine delta system: Miocene of the Eger Graben, Czech Republic. *Sedimentology*, **55**, 1419–1447.

RAJCHL, M., ULIČNÝ, D., MACH, K. & HUBATKA, F. (2003b) Large-scale stratigraphic geometries in a rift-margin, lacustrine delta system influenced by peat compaction: Comparison of field and reflection seismic data (the Miocene Bílina Delta, Ohře Rift, Czech Republic). Proceedings of the 5th meeting of the Czech Tectonic Studies Group. *GeoLines*, **16**, 87.

REITER, F. & ACS, P. (2002) Tectonics FP, Software for Structural Geology written by Franz Reiter and Peter Acs for Microsoft Windows. http://www.tectonicsfp.com.

RING, U., BETZLER, C. & DELVAUX, D. (1992) Normal Vs Strike-Slip Faulting during Rift Development in East-Africa - the Malawi Rift. *Geology*, **20**, 1015–1018.

ROJÍK, P. (2004) Tektonosedimentární vývoj sokolovské pánve a její interakce s územím Krušných hor. PhD thesis, Charles University, Prague.

SCHECK, M., BAYER, U., OTTO, V., LAMARCHE, J., BANKA, D. & PHARAOH, T. (2002) The Elbe fault System in North Central Europe-a basement controlled zone of crustal weakness. *Tectonophysics*, **360**, 281–299.

SCHLISCHE, R.W., WITHJACK, M.O. & EISENSTADT, G. (2002) An experimental study of the secondary deformation produced by oblique-slip normal faulting. *AAPG Bulletin*, **86**, 885–906.

SCHOLZ, C.A. (1995) Deltas of the Lake Malawi Rift, East Africa: seismic expression and exploration implications. *AAPG Bull.*, **79**, 1679–1697.

SCHRÖDER, B. (1987) Inversion tectonics along the western margin of the Bohemian Massif. *Tectonophysics*, **137**, 93–100.

SCHUMACHER, M.E. (2002) Upper Rhine Graben: role of preexisting structures during rift evolution. *Tectonics*, **21**, doi:10.1029/2001TC900022.

SCLATER, J.G. & CHRISTIE, P.A.F. (1980) Continental stretching: an explanationof the post Mid-Cretaceous subsidence of the central North Sea basin. *J. Geophys. Res.*, **85**, 3711–3739.

SHRBENÝ, O., BŮŽEK, Č., ČTYROKÝ, P., FEJFAR, O., KONZALOVÁ, M., KVAČEK, Z., MALECHA, A., ŠANTRŮČEK, P. & VÁCL, J. (1994) Terciér českého masívu. In: *Geologický atlas České republiky stratigrafie* (Ed. by J. Klomínský) ČGÚ, Praha. 3 pp.

SOURIOT, T. & BRUN, J.P. (1992) Faulting and block rotationin the Afar triangle, East Africa: the Danakil "crank-arm" model. *Geology*, **20**, 911–914.

SPERNER, B., OTT, R. & RATSCHBACHER L, . (1993) Fault-striae analysis: a turbo pascal program package for graphical presentation and reduced stress-tensor calculation. *Comput. Geosci.*, **19**, 1361–1388.

ŠPIČÁKOVÁ, L., ULIČNÝ, D. & KOUDELKOVÁ, G. (2000) Tectono-sedimentary evolution of the Cheb Basin (NW Bohemia, Czech Republic) between Late Oligocene and Pliocene: a preliminary note. *Stud. Geophys. Geodaet.*, **44**, 556–580.

TEODORIDIS, V. & KVAČEK, Z. (2006) Complex palaeobotanical research of deposits overlying the main coal seam (Libkovice and Lom Mbs.) in the Most Basin (Czech Republic). *Bull. Geosci.*, **81**, 93–113.

TRON, V. & BRUN, J.-P. (1991) Experiments on oblique rifting in brittle–ductile systems. *Tectonophysics*, **188**, 71–84.

TYRÁČEK, J. (2001) Upper Cenozoic fluvial history in the Bohemian Massif. *Quatern. Int.*, **79**, 37–53.

TYRÁČEK, J., WESTAWAY, R. & BRIDGLAND, D. (2004) River terraces of the Vltava and Labe (Elbe) system, Czech Republic, and their implications for the uplift history of the Bohemian Massif. *Proc. Geologists Assoc.*, **115**, 101–124.

ULIČNÝ, D. & RAJCHL, M. (2002) Reinterpretace reflexně seismických dat z mostecké pánve: Nový pohled na sedimentární výplò a deformaci uhlonosné riftové pánve. *Závěrečná zpráva o realizaci zakázky MŽP č. OG-13/02.*

ULIČNÝ, D., RAJCHL, M., MACH, K. & DVOŘÁK, Z. (2000) Sedimentation and synsedimentary deformation in a rift-margin, lacustrine delta system: the Bílina Delta (Miocene), Most Basin. Proceedings of the 5th meeting of the Czech tectonic Studies Group. *GeoLines*, **10**, 84–95.

ULRYCH, J., PIVEC, E., LANG, M., BALOGH, B. & KROPÁČEK, V. (1999) Cenozoic intraplate volcanics rock series of the Bohemian Massif: a review. *Geolines*, **9**, 123–129.

VÁNĚ, M. (1961) Příspěvek k litostratigrafické pozici salesijských křemenců v severočeské hnědouhelné pánvi. *Čas. Min. Geol.*, **3**, 346–355.

VÁNĚ, M. (1985a) Geologická stavba podkrušnohorského prolomu a jeho tektonogeneze. *Sbor. geol. Věd, Geol.*, **40**, 147–181.

VÁNĚ, M. (1985b) Geologické poměry neogenních hlavačovských štěrkopísků mezi Rakovníkem a Holedečem. *Sborn. Severočes. Muz.-Přír. Vědy*, **14**, 205–218.

WALTHAM, D. (2001) Decompact.xls. http://www.gl.rhul.ac.uk/sedtec/spreadsheets/

WILSON, M. & DOWNES, H. (1992) Mafic alkaline magmatism associated with the European Cenozoic rift system. *Tectonophysics*, **208**, 173–182.

WILSON, M. & DOWNES, H. (2006) Tertiary–Quaternary intraplate magmatism in Europe and its relation to mantle dynamics. In: *European Lithosphere Dynamics* (Ed. by R. Stephenson & D. Gee), Geol. Soc. Lond. Memoir., **32**, 147–166.

WITHJACK, M.O. & JAMISON, W.R. (1986) Deformation produced by oblique rifting. *Tectonophysics*, **126**, 99–124.

WITHJACK, M.O., OLSON, J. & PETERSON, E. (1990) Experimental models of extensional forced folds. *AAPG Bull.*, **74**, 1038–1054.

ZELENKA, O. & POLICKÝ, J. (1964) Písčité sedimenty v nadloží hnědouhelné sloje severočeského terciéru v okolí Teplic v Čechách. *Čas. Min. Geol.*, **9**, 413–420.

ZEMAN, J. (1988) Charakter neotektonické morfostruktury Krušných hor a model jejího vzniku. *Věst. Ústř. Úst. Geol.*, **63**, 333–342.

ZIEGLER, P.A. (1990) *Geological Atlas of Western and Central Europe* (pp. 1–239. Shell Internationale Petroleum Maatschappij, The Hague.

ZIEGLER, P.A. & DÈZES, P. (2007) Cenozoic uplift of Variscan Massifs in the Alpine foreland: timing and controlling mechanisms. *Global Planet. Change*, **58**, 237–269.